UNIVERSITY OF OKLAHOMA

GRADUATE COLLEGE

SPATIAL ANALYSIS OF DROUGHT AND ITS IMPACTS IN THE CHICKASAW NATION

A THESIS

SUBMITTED TO THE GRADUATE FACULTY

in partial fulfillment of the requirements for the

Degree of

MASTER OF SCIENCE IN GEOGRAPHY

By

MELISSA JAYNE WAGNER
Norman, Oklahoma
2018

SPATIAL ANALYSIS OF DROUGHT AND ITS IMPACTS IN THE CHICKASAW NATION

A THESIS APPROVED FOR THE
DEPARTMENT OF GEOGRAPHY AND ENVIRONMENTAL SUSTAINABILITY

BY

_____
Dr. Renee McPherson, Chair

_____
Dr. Hernan Moreno

_____
Dr. Mark Shafer

Acknowledgements

I would first like to thank my amazing advisor, committee chair, and mentor, Dr. Renee McPherson, for her constant support, encouragement, and guidance throughout my graduate career. She has provided me with endless opportunities to grow both academically and professionally, and there are not enough words to express how grateful I am for the help she offered these last two years. I am lucky to have worked with this influential and inspiring woman. I would also like to acknowledge the other members of my thesis committee, Dr. Mark Shafer and Dr. Hernan Moreno, for providing inspiration, reassurance and the important information that shaped my thesis into what it is today.

In addition, I would like to express my gratitude to the multiple sources of funding that have supported me through my career as a graduate student. First I would like to thank Jack Friedman for not only supporting me on the VORTEX-SE project (NOAA grant NA16OAR4590223), but also for being a wonderful mentor over the last two years. I would also like to thank the South Central Climate Adaptation Science Center for funding the last year of my research, providing opportunities to present my research at national conferences, and supporting my growth as an early career scientist. It has been a pleasure to work with everyone at the SC CASC.

Finally, I would like to recognize all of my family and friends that have helped me through this exciting period of life, and none of this would have been possible without the encouragement of partner Lance. Thank you to everyone who supported me, laughed with me, and provided me with all the love and snacks I needed to finish my thesis.

Table of Contents

List of Tables

List of Figures

Abstract

In the south central United States, drought is a prevalent natural disaster, and its impacts extend much farther than its drain on the region's natural resources. Unfortunately, local impacts of drought may differ spatially such that similar atmospheric conditions lead to different hydrologic impacts from community to community. In addition, spatial variations in drought intensity may be smaller than the size of a climate division, resulting in climate division-scale drought indices being inadequate. This study provides a spatial analysis of the impacts of drought within the Chickasaw Nation in south central Oklahoma. The goal of this study is to determine if drought was better represented by the Standardized Precipitation Index (SPI) or the Standardized Precipitation Evapotranspiration Index (SPEI) on 1-, 3-, and 12-month time scales with any spatial or seasonal differences, to see if climate-division scale data is representative of the localized impacts, and to understand how drought impacts the hydrologic resources across this study region. This study uses SPI and SPEI calculated using Oklahoma Mesonet stations within the tribal nation, and compared them to the U.S. Drought Monitor to assess the quality of the data. This was repeated for Climate division-scale SPI and SPEI to observe any differences in drought representation. Next, interpolated values of SPI and SPEI were used to distinguish any temporal, spatial, and seasonal patterns. Finally, through a case study of the 2011 – 2015 drought, this study investigated the hydrologic impacts of drought by comparing SPI and percentage of normal streamflow across the region, and calculating temporal cross correlations to distinguish any relationships between the two time series.

Chapter 1: Introduction

Drought is one of the most devastating natural disasters to plague the United States, costing cities, states, and federal government billions of dollars every year. For example, it is estimated that the 2012 drought that impacted the central United States cost the agriculture industry alone $30 billion dollars (Smith and Matthews 2015). These expensive impacts strain federal, state, and local resources, affect multiple economic sectors, and place stress on individuals and their livelihoods. The average number of billion-dollar disaster events has nearly doubled in the last five years (NCEI 2018), and with the changing climate, communities are expecting more frequent natural hazards, including drought. According to the U.S. Global Change Research Program's (2014) National Climate Assessment, the number of consecutive dry days is expected to increase by 2-4 days across the Great Plains in both the higher and lower emission scenarios, and periods of intense drought are projected to become more frequent in the southern Great Plains region (NCA 2014). These projected changes will prove to be difficult for decision makers faced with tough decisions when dealing with drought.

Making decisions to prepare for, manage, and control the impacts of drought is a daunting task for city, state, and federal leaders. The U.S. 2017 Billion-Dollar Weather and Climate Disasters assessment (NCEI 2018) reported 16 billion-dollar disasters, costing over $300 billion dollars total, with drought being one of the 16 the billion-dollar events. Still, Smith and Matthews (2015) found that the estimated average financial impact of disasters was underestimated by 10-15% especially with drought. This estimation discrepancy was due to uncertainty in specific impacts of each drought, and the growing problem that there is a great deal of uncertainty when it comes to

estimating the financial losses due to drought impacts (Smith and Katz 2013). This ambiguity is a major problem for managers and decision makers planning for these types of events — a problem that can be exacerbated when they are faced with limited resources or when data are not available.

The local impacts of each drought are unique —whether from the spatial variability of the drought's severity or from local-level mitigation, response, or recovery decisions. Many smaller communities are not equipped to handle the overbearing impacts of these large-scale disasters, and the uncertainty in how a drought affects their specific jurisdiction and resources presents an additional problem for decision makers. In addition, the spatial variability of the duration and intensity of any given drought is determined by many geographical and climatic factors, such as urbanization, air temperature, or hydrologic resources present. These factors cause feedbacks that affect the intensity of those droughts (Rim 2013). Unfortunately, this spatial variability in the physical conditions of the landscape is difficult to capture in drought indices without the appropriate resolution data set. While many indices are now produced at a station-based scale, many are still calculated on a climate-division scale; thus, they do not have the resolution to compare to localized drought impacts.

How different institutions and jurisdictions plan for and respond to drought also plays a vital role in how a drought affects one community versus another. One challenge faced is the difficulty connecting the impacts in a specific area to the drought information needed to make decisions to plan and respond to the impacts of drought (Towler and Lazrus 2016). In addition, the physical impacts of drought have a direct effect on many of the socio-economic concerns faced during times of drought (Wheaton

et al. 2008). Societal vulnerability to drought impacts is a factor of the severity of the drought itself and the stress placed on the natural resources used by that society (Wilhite et al. 2007). It was found that the frequency of drought events in a particular area can influence the overall impacts felt by a community. In addition, the initial condition of hydrologic resources before the drought and the deficit in these resources play a major role in the severity of these impacts (Soulé 1992). Overall, the complexity of the stakeholder decision-making process depends on the spatial variability of the drought itself, the decision-making process of the managers in that region, and the diverse impacts felt by that community.

To better understand the challenges faced when analyzing the spatial variability of drought in a region, we conducted a spatial analysis of drought and its impacts across south-central Oklahoma. This spatial analysis investigates the significance of using drought indices on a finer resolution to assess the physical impacts of drought on the water resources in the region. First, we calculated two drought indices on a fine spatial resolution — the Standardized Precipitation Index (SPI) and the Standardized Precipitation Evapotranspiration Index (SPEI) — in order to analyze the spatial variability of drought within this region. These values are then compared to values from the U.S. Drought Monitor, a drought-monitoring tool that combines physical drought indices and impacts, over the same region. Next, we analyzed the hydrologic impacts during times of drought. The rivers, lakes, springs, and ground water are highly variable, and these resources serve as a long-term example of competing needs and climatic stresses. To better understand these impacts, we conducted a case study of the 2011-2015 drought to compare the hydrologic deficits to our calculated drought indices.

.

1.1 Study Area

The study area for this project encompasses the 13 counties of The Chickasaw Nation. In recent years, The Chickasaw Nation and its people have suffered from severe to exceptional drought conditions, leading them to partner with The Choctaw Nation of Oklahoma on drought planning. Because the territorial boundaries of The Chickasaw Nation are similar to the size of a climate division, and because a high-density climate observation network overlies their territory, we chose to use this region for our research.

The history of The Chickasaw Nation began long before European settlement in North America. The Chickasaws originated in what is now known as northern Mississippi, Alabama, and southern Tennessee, with records of their physical presence in the area dating back 12,000 to 16,000 years ago. From early settlement, both the French and the English fought with The Chickasaw Nation to steal their land until eventual removal of their people in 1837-38 to Indian Territory (now Oklahoma; Babb 2015; Malone 1922). The boundaries of the Nation that we know today were established by the Treaty of Washington in 1855 in what is now south-central Oklahoma. This sovereign, self-governed Nation has played a vital role in the history of the state of Oklahoma (Malone 1922). The Chickasaw Nation is a key contributor to the state's economy, with thriving tribal and non-tribal industries (Babb 2015). Figure 1 highlights the Nation's location in south-central Oklahoma, just along the northern border of Texas (Figure 1).

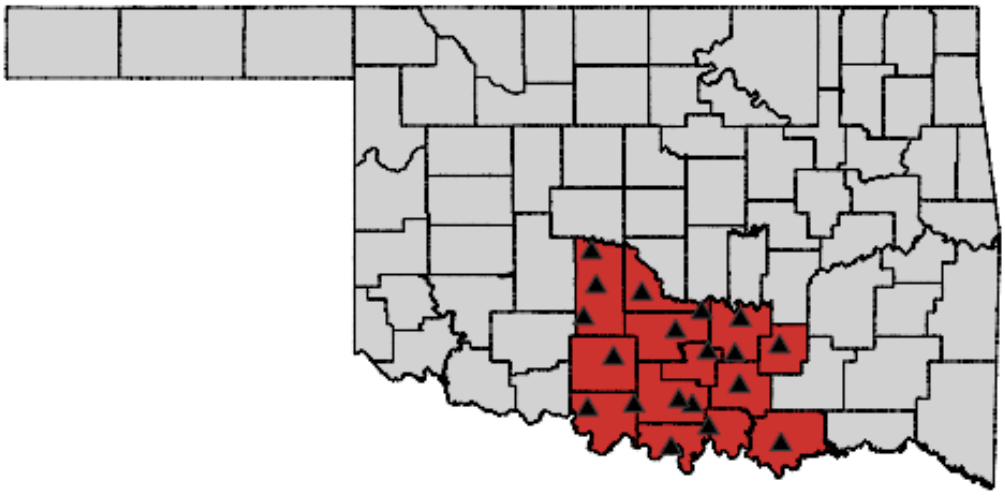

Figure 1: The Chickasaw Nation (red) within Oklahoma (grey). Locations of Oklahoma Mesonet weather stations within the Nation's boundaries are designated by solid, black triangles.

Drought has impacted nearly every economic sector within The Chickasaw Nation, including agriculture, recreation and tourism, public health, industry, and, most importantly, water resources (The Nations 2017). The area has experienced many dry periods, including droughts, over the last hundred years (Fig. 2), with the most recent multi-year drought in 2011-2015.

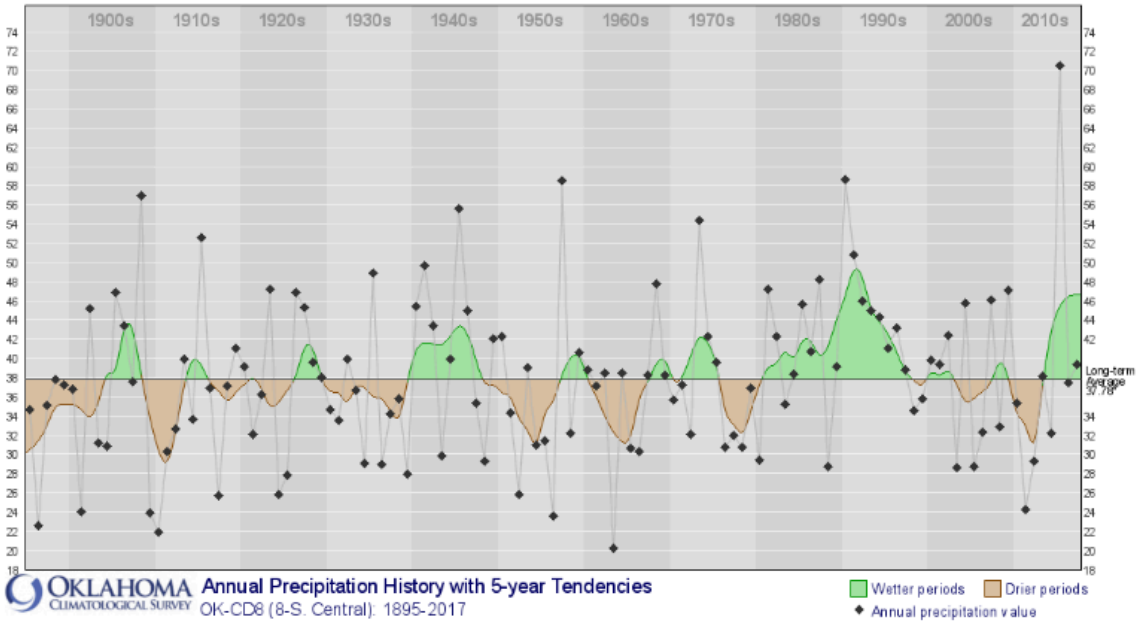

Figure 2: Annual precipitation in inches (dots) with 5-year tendencies (brown and green shading) for Oklahoma climate division 8, from 1895 - 2017 (OCS 2018).

This extended period of drought can be used to spotlight the devastating impacts drought can have on a region, a government, and its citizens. For example, the Chickasaw National Recreation Area, located in the heart of this region, was hard hit during the 2011-2015 drought. One of its major springs, Antelope Springs, stopped flowing from the summer of 2012 through spring 2015, resulting in the closure of popular swimming areas in the park (The Nations et al. 2017). In addition, Lake of the Arbuckles reached record-low levels, further impacting tourism by limited fishing and boat access throughout the lake. Decision makers were faced with concerns regarding local cities' water quality and insufficient water supply due to the lack of alternative water supplies. Communities that relied on waters from the Arbuckle-Simpson Aquifer (in east-central Chickasaw Nation) were particularly hard hit.

Another industry impacted by the 2011-2015 drought was agriculture. The lack of precipitation damaged crops and reduced plant yield, not only impacting the

agricultural producers financially, but also putting a strain on livestock and cattle that depended on this source of food (The Nations et al. 2017). The western half of the Nation was particularly devastated by cattle and crop losses, with wheat losses up to 60,000 acres from 2007 to 2012 in some counties (The Nations et al. 2017).

The motivation for this research began from discussions with employees of The Chickasaw Nation who indicated that while they saw improvement in the drought indices (e.g., Palmer Drought Severity Index, US Drought Monitor), their rivers, streams, and springs remained dry. They were concerned that climate division-scale information proved inadequate for local decisions. They asked if we could determine if higher-resolution indices would be more useful because of increased spatial variability.

Chapter 2: Literature Review

The need to accurately and efficiently monitor drought has been experienced for decades. It has long been understood that many meteorological phenomena (e.g., rainfall, high temperatures) influence the local climate, but these factors themselves do not completely describe how a surplus or deficit in moisture in an area shapes drought (Thornthwaite 1948). While there are many different definitions of drought, for the purpose of this study, we will focus on "meteorological drought," characterized by an extended period of below-normal precipitation or moisture (American Meteorological Society 2018; Palmer 1965).

Many indices and tools have been developed to monitor and better understand drought, but with a natural phenomena as complex as drought, it can be hard to link any given index or tool to local impacts. For example, Guttman (1999) explains that the Palmer Drought Severity Index (PDSI) and the Palmer Drought Index (PDI) are intended to be retrospective calculations of drought severity, and using these indices to assess spatial or temporal elements of drought could misrepresent these conditions. Currently, real-time monitoring of PDSI is only calculated on a climate-division scale, but this spatial extent does not provide the detail needed to assess drought on a community-to-community basis.

Even with the spatial coarseness of the drought indices, users have found them helpful for many types of decisions, including analyzing the effects of decreased precipitation and surface moisture on streamflow during periods of extended drought (Dai et al. 2004). Yet the abundance of different measures of drought can be daunting. As mentioned above, PDSI is a popular index that use precipitation, evapotranspiration,

and soil moisture to evaluate drought severity (Alley 1984), but potential evapotranspiration was found to have little effect on PDSI values, as those calculations correlated with soil moisture (Dai 2011). Another example is the reconnaissance drought index (RDI), which uses a ratio of precipitation to reference crop evapotranspiration to evaluate drought (Tsakiris and Vangelis 2005; Vangelis et al. 2011). RDI incorporates evapotranspiration in its calculation to investigate the link between the recurring droughts and stresses on water resources (Tsakiris and Vangelis 2005). The Normalized Difference Vegetation Index (NDVI) is another derived product used to help monitor drought; it is used to calculate the Standardized Vegetation Index, which provides a departure-from-normal vegetative conditions linked to drought (Peters et al. 2002).

The Standardized Precipitation Index has gained popularity in the last few decades, and offers a standardized index, directly related to precipitation, that has the ability to be calculated over different timescales (McKee et al. 1993). From the SPI method, another index — the Standardized Precipitation and Evapotranspiration Index — has been developed and incorporates temperature into its calculation (Vicente-Serrano et al. 2010). One of the first widely accessible drought monitoring tools was the U.S. Drought Monitor, which combines objective inputs, climate indices, numerical models, and local, subjective input from different regions across the country into a weekly map that highlights drought magnitude across the nation (Svoboda et al. 2002). We discuss several of these products in depth below.

2.1 Standardized Precipitation Index

With meteorological drought, it is important to understand how a deficit in precipitation affects the magnitude of drought, highlighting a need for a drought index that is linked to precipitation in a particular region. McKee et al. (1993) define the Standardized Precipitation Index (SPI) as:

$$SPI = \frac{(p - \bar{p})}{\sigma_p} \qquad \text{(Equation 2.1.1)}$$

where p is the standardized dataset of observed precipitation, $\bar{p}$ is the mean of the precipitation record, and σ_p is the standard deviation of the same precipitation record. They define a drought event as any period of time with continuously negative SPI values below -1.0.

Standardizing the long-term precipitation observations using a suitable probability distribution function (PDF) is a crucial step in calculating SPI. It is important to identify an appropriate PDF, such as the Pearson Type III distribution or the gamma distribution, to normalize the dataset (Edwards 1997; Guttman 1999; Hayes 2000). The process of standardizing the precipitation observation ensures that drought is relative to the local climate; that is, there may be more precipitation that occurs during a drought in a wet climate than occurs during normal conditions in a dry climate. The SPI then can provide localized information about the development and trends of drought in any given area with a sufficient precipitation record (typically more than 50 years).

SPI typically is calculated on time intervals of 1, 3, 6, 12, 24, and 48 months within a continuous precipitation data set. SPI values are calculated on a monthly basis, with a moving window of the respective time intervals, and due to the standardization of the data, each monthly SPI value is dependent on the previous month's value. When

first developed, SPI was proposed to have four drought categories: mild drought (0 to -0.99), moderate drought (-1.00 to -1.49), severe drought (-1.50 to -1.99), and extreme drought (less than or equal to -2) (McKee et al. 1993; Umran 1999). Later, the index added periods of neutral conditions or no drought (from 1 to -1) and wet periods (greater than +1) identified in the SPI time series (Agnew 2000; Guttman 1999).

2.1.1 SPI and Drought

The use of precipitation time series when calculating SPI allows users to better assess the development and severity of drought in terms of water deficit in a particular region (Vicente-Serrano et al. 2010). The simple formula and minimal data needed for calculation make SPI an excellent and easy-to-implement tool for a local scale drought study.

Raziei et al. (2009) found that spatial patterns of SPI calculated over shorter time scales (1-3 months) were observed to be consistent with local precipitation patterns. Furthermore, spatial trends over these time scales provided a link between precipitation patterns and drought evolution (Zhai et al. 2010). While some of these studies focus on the spatial variability of drought, many also included analyses that compared the calculated time scales (e.g. 1-month, 3-month, or 12-month calculations). Prior studies have utilized SPI because of its ability to monitor periods of below-normal precipitation and to directly compare wet and dry periods (Bonaccorso et al. 2003; Umran 1999). Calculations of SPI can highlight areas with consistent trends of drier periods (Bonaccorso et al. 2003; Umran 1999), identifying areas where a change in the character of drought may be occurring. As the calculated time scale increases to 12 months, longer-term trends in drought development and intensity can be extracted

(Vicente-Serrano 2006). Monitoring drought over different time scales provides a more comprehensive view of not only the intensity of drought, but also the early onset, development, and extent of drought that other indices lack (Hayes et al. 1999).

SPI has been compared to many drought indices, such as PDSI and RDI (Alley 1984; Karl 1986; Khalili 2011; Guttman et al. 1992), and used to analyze the spatial and temporal characteristics of drought across many regions. While PDSI has the ability to incorporate temperature into its calculation, it does not incorporate the functionality to calculate the index on multiple time scales that is critical when using SPI to assess drought (Palmer 1965). In addition, the standardized expression of RDI performs similarly to SPI (Tsakiris and Vangelis 2005).

In summary, one of the key features of SPI is that it directly relates to the amount of precipitation in a region, thus SPI provides a useful depiction of the meteorological drought conditions based on an over/under abundance of moisture (Guttman 1998). Another important quality of SPI is that the resolution of the index is determined by the resolution of the precipitation dataset. This feature allows users to calculate SPI using multiple precipitation datasets, which provides the opportunity to calculate the index on a higher resolution. In addition, calculating SPI over different time scales gives information on both long-term and short-term droughts.

2.2 Standardized Precipitation Evapotranspiration Index

With increasing global surface temperatures over the last 30 years and a projected increase into the future (IPCC 2014), temperature will play a major role in future droughts across North America and beyond. Higher temperatures generate increased evapotranspiration, especially during the warm season. Flash droughts, or

rapid-onset droughts can occur as deficits in precipitation are paired with increasing warm season temperatures, and can trigger near-normal conditions to deteriorate to extreme or exceptional drought conditions in just a few months (Otkin et al. 2017). With these considerations in mind, Vicente-Serrano et al. (2010) proposed a new drought index, the Standardized Precipitation Evapotranspiration Index, that accounts for both precipitation and temperature as drought indicators in order to better account for a warming climate.

To incorporate temperature into this drought calculation, SPEI includes evapotranspiration in the method for calculating SPEI (equation 2.2.1):

$$SPEI = \frac{\left((P - ET_o) - \overline{(P - ET_o)}\right)}{\sigma_{(P-ET_o)}}$$

where $(P - ET_o)$ is the difference between precipitation (P) and evapotranspiration (ET_o) — a water balance calculation, and $\sigma_{(P-ET_o)}$ is the standard deviation of the water balance (Beguería and Vicente-Serrano 2013; Beguería et al. 2014).

The American Meteorological Society (2018) defines evapotranspiration as, "the combined processes through which water is transferred to the atmosphere from open water and ice surfaces, bare soil, and vegetation that make up the earth's surface." Although actual evapotranspiration is difficult to measure directly, there are many ways to estimate potential evapotranspiration and use that value as a proxy for actual evapotranspiration. For example, Thornthwaite's equation (equation 2.2.1) is a simple calculation of potential evapotranspiration (Thornthwaite 1948),

$$PET = 16K\left(\frac{10T}{I}\right)^m \qquad \text{(Equation 2.2.1)}$$

where T is the monthly mean temperature, I is the heat index, m is a coefficient of I, and K is a correction coefficient based on the latitude and month. Similarly, Hargreaves equation (equation 2.2.2) estimates a reference crop evapotranspiration from temperature (Hargreaves and Samani 1985),

$$ET_o = 0.0135 \times RS(T + 17.8) \qquad \text{(Equation 2.2.2)}$$

where T is the temperature in degrees Celsius and RS is solar radiation. The Penman-Monteith equation (equation 2.2.3) is a more complicated equation using not only temperature, but also solar radiation, wind speed, and relative humidity, to calculate reference evapotranspiration (Allen et al. 1994),

$$\lambda ET = \frac{\Delta(R_n - G) + \rho C_p (e_a - e_d)/r_s}{\Delta + \gamma\left(1 + {}^{r_s}/_{r_a}\right)} \qquad \text{(Equation 2.2.3)}$$

where λ is the latent heat of vaporization, R_n is net radiation from the atmosphere, G is sensible heat from the soil, Δ is the slope of the saturation pressure-temperature relationship, ρ is the mean air density, C_p is the specific heat capacity of air, γ is the psychrometric constant, r_s is the bulk surface resistance, r_a is the bulk aerodynamic resistance, and $e_a - e_d$ is the vapor pressure deficit of the air. In all of these cases, the SPEI calculation assumes that actual evapotranspiration is close to potential evapotranspiration — an assumption that rarely holds during drought conditions.

There is a high correlation between SPI and SPEI, especially in cool climates or during cool winters due to the minimal impact of temperature in SPEI's water balance calculation; however, this correlation decreases when the indices are calculated in locations where the temperature has increased over long time scales (decades to centuries) (Vicente-Serrano et al. 2010).

2.2.1 SPEI and Drought

SPEI is still a relatively new drought index, with not as many case studies in the literature as there are for SPI. Because SPEI can account for the projected warming in a changing climate, it allows the user to better understand how increasing temperatures affect drought severity (Vicente-Serrano et al. 2010). The literature agrees that SPEI is a good choice for investigating future climate change effects, as SPI cannot identify increases in drought duration, intensity, and magnitude resulting from rising global temperatures (Begueria et al. 2014, Vicente-Serrano et al. 2010, and Zargar et al. 2011). Potop (2011) found that there are seasonal variations when evaluating SPEI, concluding that increased temperature anomalies during the warm seasons, and thus increased PET values, influenced both the severity and duration of persisting drought. Furthermore, inclusion of PET (i.e., water balance) in the evaluation of drought magnitude gives insight to the drought impacts on ecological and hydrological systems in an area (Vicente-Serrano et al. 2012). When comparing SPI and SPEI, it was found that temperature played a significant role when analyzing the impacts of drought on hydrologic variables (Lorenzo-Lacruz et al. 2010).

The relationship between temperature and drought severity provides additional information that can be critical for decision makers during times of drought. Unfortunately, this index is still relatively new in the field of drought monitoring; little research has been conducted analyzing the spatial and temporal variability of SPEI. The incorporation of evapotranspiration, or more importantly temperature, may prove to be very useful in the future as decision makers and stakeholders consider drought in our warming climate.

There are many applications of these drought indices, each lending insight to their failures and successes. SPI has long been used to analyze spatial and temporal patterns of drought, but since SPEI is relatively a new index, there is little evidence to compare the two. SPI and SPEI were found to perform similarly when analyzing spatial trends in drought, but SPEI was more sensitive to long-term trends in temperature (Zargar et al. 2011). While SPI and SPEI highlighted similar spatial trends in drought, temperature provided additional information that played a significant role when analyzing the impacts of drought on hydrologic variables across the region (Lorenzo-Lacruz et al. 2010). Additionally, SPI can be used to emphasize the complex nature of the spatial variability of drought, and over long time scales (12-, 24-, 48-months), the variability between drought and the climatic variables decreases (Vicente-Serrano 2006).

2.3 Drought Monitor

The U.S. Drought Monitor (USDM) was developed out of a need for a better method of monitoring drought conditions across the United States. Svoboda et al. (2002) explain that the USDM is in fact not a drought index, but a drought monitoring tool created to provide decision makers a comprehensive drought-monitoring summary that combines objective inputs including six physical indicators (PDSI, Climate Prediction Center Soil Moisture Model Percentiles, Daily Streamflow, Percent Normal Precipitation, SPI, and Satellite Vegetation Health Index), climate indices (temperature, precipitation), and analysis tools (such as the Objective Blend of Drought Indicators, Soil Climate Analysis Network). USDM authors also incorporate subjective content, such as feedback from climate professionals from different regions across the country.

In addition, USDM uses SPI as one of the objective indicators when considering drought categories. The USDM also takes into account the USGS Weekly streamflow percentiles when evaluating drought indicators and assigning its drought categories, and this impacts-based approach made the USDM a suitable fit for evaluating the physical impacts of drought. This drought-monitoring tool is useful when investigating the impacts of drought across a region because it is intended for the evaluation of drought impacts.

The authors express that the USDM is a unique drought classification scheme that allows the user to assess both the intensity and spatial extent of drought across their region (Svoboda et al. 2002). Each drought category is assigned based on the 100-year percentile chance standardized by time of year (Svoboda et al. 2002), as follows:

Table 1: U.S. Drought Monitor (USDM) categories (left) with percentile thresholds (right) (Svoboda et al. 2002)

USDM Category	USDM Description	Percentile
D0	Abnormally dry	20 to ≤ 30
D1	Moderate drought	10 to ≤ 20
D2	Severe drought	5 to ≤ 10
D3	Extreme drought	2 to ≤ 5
D4	Exceptional drought	≤ 2

To evaluate the severity of drought, USDM assigns the thresholds of each drought category to a percentile of frequency of historical occurrence. An operational USDM map has been released weekly since 2000 that highlights areas, intensity, and impacts of drought (USDM 2018(a)). Additional, associated products include drought summaries for seven regions across the county (Northeast; Southeast; South; Midwest; High Plains; West; and Alaska, Hawaii, and Puerto Rico) and county-level, state-level, and regional

data (free of charge on the USDM website at http://droughtmonitor.unl.edu/) in GIS format, as well as regional or state-level maps and drought summaries.

2.3.1 Drought Monitor and Drought

USDM incorporates many of the crucial characteristics needed to properly define types of drought, including geographic extent, duration, and severity (Zargar et al. 2011). Because the current USDM values are displayed on a map every week, it provides spatial context to the current condition of drought across the country, but is not intended to replace the knowledge of local decision makers (Heim Jr. 2002). The success of the USDM has led to the larger, multinational monitoring program called the North America Drought Monitor (NADM) that provides drought monitoring and synthesizing drought indicators across Canada, Mexico, and the United States (Lawrimore et al. 2002; NOAA 2018). Some limitations to the USDM include its inability to portray the temporal components in drought development and intensity, and the fact that USDM does not illustrate drought magnitude beyond the borders of the United States (Hayes et al. 2011; Heim Jr. 2002). Also, a big criticism is that it does not distinguish between *types* of drought such as agricultural versus hydrological drought.

Many studies have used USDM for comparison to drought indices. Through a comparison of different drought indices and drought monitoring tools, the authors stress that while the USDM provides a good way to indicate sectors that are being affected by drought, it is limited in its ability to provide temporal information on the development of drought (Mishra and Singh 2010). Peters et al. (2002) utilized USDM maps to measure the accuracy of their interpolated values of Normalized Difference Vegetation Index (NDVI) Standardized Vegetation Index across their study area, and to verify their

representation of drought severity. Similarly, USDM has been used to examine the spatial variations in the remotely sensed NDVI Vegetation Health Index (Rhee and Carbone 2010).

2.4 Hydrologic Indices

Hydrology is the "occurrence, distribution, movement, and properties of the waters on the earth," and its interactions with the environment are controlled by the physical processes encapsulated in the hydrologic cycle (Viessman et al. 1989). Hydrologic data are defined to include information regarding variables such as streamflow, evaporation, transpiration, runoff, and soil moisture, along with their interaction with climatological data like rainfall, snowfall, humidity, and solar radiation (Viessman et al. 2013). There are hundreds of hydrologic features within the Chickasaw Nation, including rivers, major and minor streams, lakes, springs and aquifers. River discharge, groundwater levels, soil moisture, and other hydrologic variables have long been used to assist in determining the severity of drought in a particular location (Palmer 1965). In addition, the analysis of different hydrologic indices allows us to examine the magnitude of the drought, or the threshold of the moisture deficit throughout the period of drought, across that region (Zargar et al. 2011). While there are monitoring stations within the study area that measure many hydrologic variables, this review will focus on streamflow. Streamflow, or discharge, is defined by a volume of open flow of water per unit time from any natural or open channel, or discharge. Streamflow can change through water's interaction with the hydrologic and geologic structures within the study area.

The distinctive hydrogeologic structure is one of the factors that make the monitoring the water resources in south-central Oklahoma such a challenge. A fundamental supplier of flow to many of the rivers, streams, and springs in our study area is the Arbuckle-Simpson Aquifer, spanning more than 500 square miles beneath five of the Nation's 13 counties (OWRB 2018). Around 150,000 residents from dozens of cities, towns, and rural water districts obtain their water from the Arbuckle-Simpson Aquifer, and in the majority of cases, this aquifer is the only source of ground water for those consumers and the primary source of drinking water for one of the most populated municipalities in the region — Sulphur, OK (Choctaw and Chickasaw Nations et al. 2017).

The Arbuckle-Simpson Aquifer was designated by the Environmental Protection Agency (EPA) as a Sole Source Aquifer, which adds protections to this region's limited drinking water (The Choctaw and Chickasaw Nations et al. 2017). The U.S. Environmental Protection Agency (EPA 2006) defines a Sole Source Aquifer as, "an aquifer that supplies 50-percent or more of the drinking water of an area." This resource is particularly vulnerable due to the fact that the only recharge mechanism is from precipitation, and below-normal precipitation results in below-normal recharge for the aquifer. There has been a lot of success modeling this aquifer, along with many of the associated rivers and streams, to better understand how meteorological variables (such as precipitation) influence the various hydrologic processes (runoff, infiltration, streamflow, or subsurface flow). These modeling efforts combined with improved understanding of additional influences such as human extraction, impediments, and diversions, help scientists to better comprehend the complex subsurface geologic

system dominating the area (Christenson et al. 2011; Faith et al. 2010; Looper et al. 2012). Recognizing the hydrologic processes that are influencing the water resources within this region provides crucial details about how these resources will react when the water resources are strained during drought.

2.4.1 Hydrologic Indices and Drought

As our climate changes, increasing temperature and variations in precipitation patterns are expected to influence the hydroclimate, leading to areas of increased or decreased streamflow into the year 2050 (Milly et al. 2005). Anthropogenic influences on hydrologic indices are changing the previously assumed stationarity in the hydroclimate, and it is driving the hydrologic conditions past its historical bounds (Milly et al. 2008). These projected changes will influence how water resources interact with the landscape, and the variability is expected to influence the drought vulnerabilities across the globe. Changes in the environment like these make studying the impacts of drought that much more important.

The Chickasaw Nation has many drought vulnerabilities, ranging from hydrologic infrastructure issues to increased municipal growth and demand in the region, with the most significant vulnerability being an insufficient and/or unreliable supply of water. This strain on hydrologic resources during periods of drought negatively impacts a wide variety of stakeholder groups including private landowners, tourism and recreation, agriculture, and energy (The Nations et al. 2017). The immense impact of drought within the Nation prompted a $400,000 program between the Bureau of Reclamation and the Choctaw (of Oklahoma) and Chickasaw Nations to develop a Drought Contingency Plan (DCP) for the Arbuckle Simpson Aquifer. The DCP task

force assigned three stages of drought based on five hydrologic triggers: Arbuckle Lake level, USGS Fittstown monitoring well depth, Antelope Springs springflow, USGS Blue River streamflow, and PDSI for Oklahoma Climate Division 8.

Table 2: Drought Triggers designated by the Arbuckle-Simpson Aquifer Drought Contingency Plan (The Nations et al. 2017)

Triggers	Thresholds
Arbuckle Lake:	The water level in Arbuckle Lake drops below 867 feet (five feet below conservation pool elevation)
Fittstown Well:	Depth to water in the USGS Fittstown monitoring well drops below 120 feet
Antelope Springs:	Flow in Antelope Springs drops below 0.5 cfs
Blue River:	Flow in the Blue River near Connerville drops below 33 cfs
Palmer Drought Severity Index (PDSI):	The PDSI for Oklahoma Climate Division 8 drops below -4.0 (Extreme Drought)

Table 3: Drought Stages and corresponding conditions necessary to prompt response action as designated by the Arbuckle-Simpson Aquifer Drought Contingency Plan (The Nations et al. 2017)

Drought Stage	Conditions necessary
Drought Stage 1 (Alert):	Any one of the five thresholds is reached
Drought Stage 2 (Warning):	All five of the thresholds are reached
Local Drought Stage 3 (Emergency):	Dictated by local conditions

The actions based on the thresholds set by the DCP are determined monthly, and the response action is determined by drought stage and sector (The Nations et al. 2017). For example, a "stage 2 – warning for the energy sector (oil and gas)" would result in a response action of reducing potable water use by 40 percent (The Nations et al. 2017). Research on these "drought triggers" is beneficial for drought monitoring in this region, leading to vital information for decision makers to plan for drought in the future.

There are a multitude of drought triggers that can be observed and studied; each trigger can capture an important feature in how hydrologic variables behave during times of drought in a specific region. Because SPI and SPEI are directly related to precipitation, researchers have investigated how these indices relate to hydrologic responses, such as runoff amounts, lake level changes, or soil moisture depletion. For example, Fiorillo and Doglioni (2010) used a cross correlation analysis between rainfall and karst aquifer spring discharge, and found that rainfall correlates with discharge over longer time periods (>10 days), with the strongest correlation observed for 150 to 270 day periods. Zhai et al. (2010) found that there was a significant correlation between SPI and the percentage of runoff anomaly in river basins in China. In addition, a study of the relationship of drought indices and spring discharge from a karst aquifer revealed that extended periods of below average rainfall not only leads to an initial decrease in discharge from springs and rivers, but also results in long term effects on the aquifer (Fiorillo and Guadagno et al. 2010).

Furthermore, SPI and SPEI are beneficial to use when considering water resources because of their ability to be calculated on different timescales, allowing decision makers to better assess the severity (Hayes et al. 1999). Longer time scales of SPI, such as 12, 24, or 48 months, can better identify impacts on long-term hydrologic resources, such as aquifers (Fiorillo and Guadagno, 2010; Vicente-Serrano 2006). The footprint of a multi-year drought can last well beyond the time frame that climatic variables return to normal. For example, Tang and Piechota (2009) concluded that that a one-year, post-drought period with positive soil moisture anomaly did not allow for drought recovery from a four-year drought period. The connection between drought and

hydrologic resources can be a challenging for decision makers to understand if they do not have the information necessary to look at the whole picture when it is concerning drought.

Within Oklahoma, the impacts of drought can vary widely. Illston and Basara (2003) found that there were many spatial and temporal variations in short-term drought (defined as less than six months) across Oklahoma, with extremely dry soil moisture conditions varying seasonally during different periods of drought, and occurring over various seasonal precipitation patterns. The authors assert the importance of calculating drought on shorter time scales. However, there were limitations to their analysis of the localized impacts; PDSI and SPI did not have the ability to incorporate the extreme temperature that occurred during their time frame, and both of these indices were calculated on a climate division scale which lead to reduced spatial resolution when analyzing these indices (Illston and Basara 2003).

Chapter 3: Data and Methods

This study provides a spatial analysis of drought and its impacts within the Chickasaw Nation. The research overviewed in chapter 2 indicated that several ways to monitor drought currently exist. Each method has its benefits and limitations, and most methods have been used extensively by decision makers to track ongoing drought conditions. Local impacts of drought, however, may differ spatially such that similar atmospheric conditions lead to different hydrologic impacts from community to community. In addition, spatial variations in drought intensity may be smaller than the size of a climate division, resulting in climate division-scale drought indices being inadequate in some cases.

To examine this spatial variation of drought and its impacts, we ask the following questions:

- Is the drought severity across the study region better represented with SPI or SPEI on one-, three-, or 12-month scales? Is there a spatial or seasonal component to the differences in how these six indices (SPI 1-month, SPEI 1-month, SPI 3-month, SPEI 3-month, SPI 12-month, and SPEI 12-month) represent drought severity?
- Are SPI and SPEI, calculated on a climate-division scale, representative of the localized impacts in the study region?
- How does drought impact the hydrologic resources from community to community across this study region?

To answer these questions, we utilized the following study region, datasets, and methods.

3.1 Domain

The Chickasaw Nation encompasses 13 counties within south-central Oklahoma. Within these boundaries, there are 19 Oklahoma Mesonet stations and 23 hydrologic observing stations, discussed in depth below. Because of a significant west-to-east precipitation gradient and the Arbuckle Anticline, the region's physical geography is diverse.

Under the Köppen-Geiger climate classification system (Köppen 1936), the entire region has a humid subtropical climate (Cfa) — a temperate climate with warm, humid summers and mild winters (Peel et al. 2007). Although the region is one climate classification, there is diversity in its atmospheric conditions. The precipitation in the region is highly variable, with normal precipitation values ranging from 750 mm (northwest) to 1125 mm (southeast) annually (OCS 2018; Fig 3). Annual average temperatures range from 15° C along the northern border of the Nation to 17° C on the southern border (OCS 2018; Fig. 3).

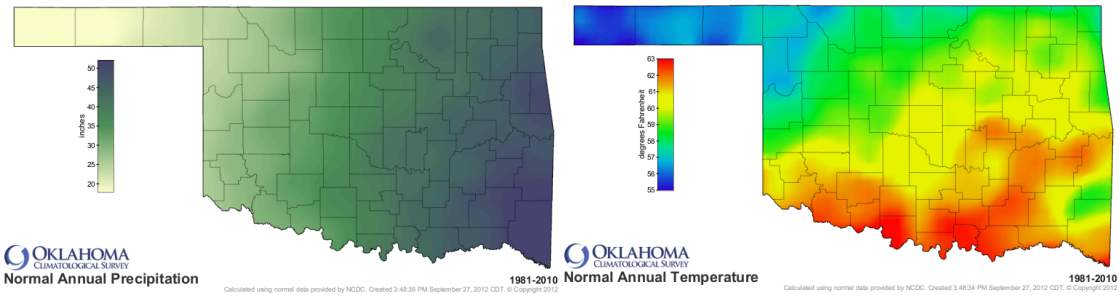

Figure 3:Normal Annual Precipitation, in inches (left) and Normal Annual Temperature in Fahrenheit (right) over a 30-year period (1981-2010) (OCS 2018).

Furthermore, there is quite a variance in physical landscape and geologic structure across the region. The landscapes in and around the Arbuckle-Simpson Aquifer contain areas of rocky limestone, dolomite, and granite features in the Arbuckle

Mountains. The region contains many natural springs, caves, and streams resulting from this karst topography. Outside of the Arbuckle Anticline there are regions of rangelands and grasslands with sandier soils of shale and sandstone (Christenson et al. 2011; EPA 2018; Faith et al. 2010).

The hydrologic conditions within the Chickasaw Nation have long been a critical issue because of the demands on the watershed's limited water supply (The Nations et al. 2017). The area's many springs are dependent on the karst Arbuckle-Simpson aquifer (OWRB 2003), as well as hundreds of rivers and streams that traverse across the region. Understanding how these resources fluctuate during times of drought is of high importance for the Chickasaw Nation, as sectors within the region such as agriculture, recreation, and tourism are highly dependent on the condition of their hydrologic resources (The Nations et al. 2017). Because precipitation serves as the primary recharge mechanism, surface and below-ground water resources are highly dependent on its variability across the region, highlighting the complicated relationship between precipitation and the hydrologic resources. The link between precipitation, hydrologic resources, and drought impacts in this region are why we decided to investigate these variables in our spatial analysis of drought in this region.

The region is home to many plant and animal species, with five different ecoregions present across the landscape (EPA 2018; Fig. 4). The majority of the study area is designated as the Cross Timbers ecoregion, stretching from the northern to southern border. The ecoregion transitions along western edge of the Chickasaw Nation to the Central Great Plains ecoregion. Adding to the diversity of the region, the southeastern corner of the study area has a more varied ecological landscape, with East

Central Texas Plains, South Central Plains, and Arkansas Valley ecoregions weaving through the region (EPA 2018).

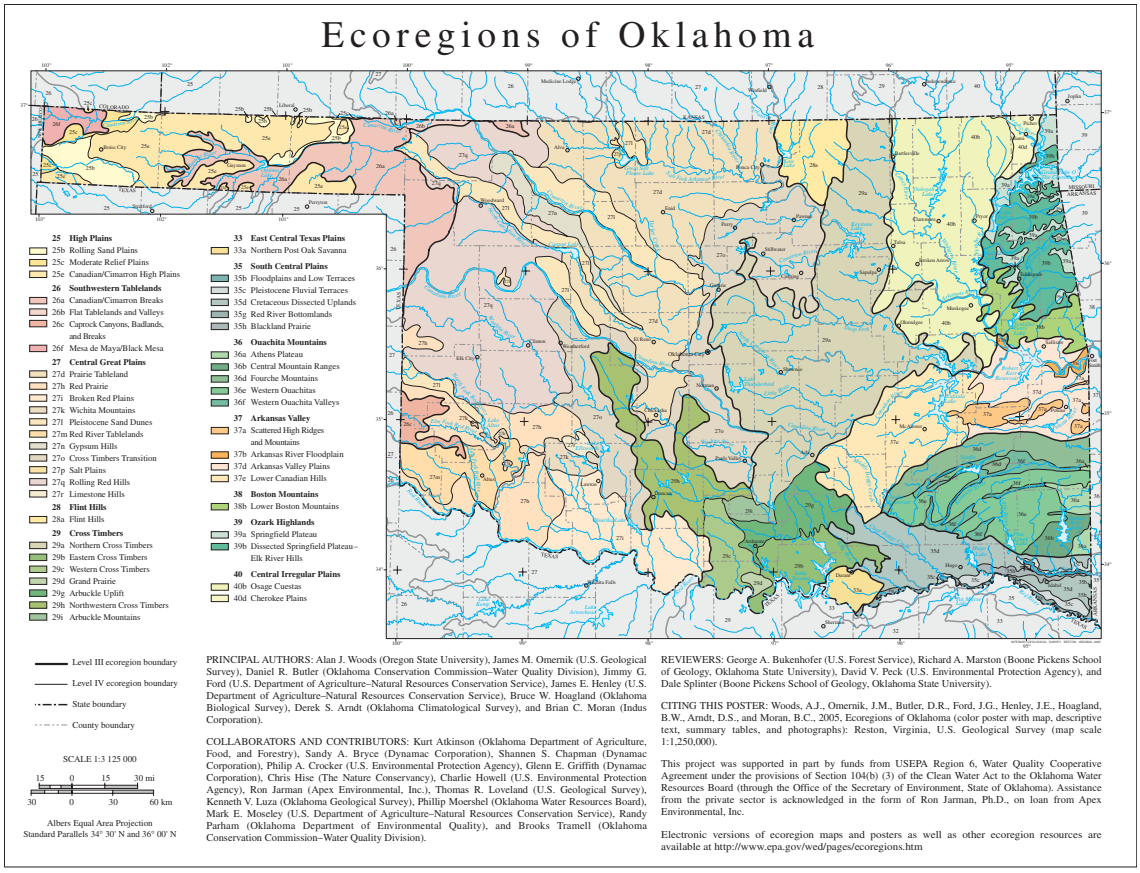

Figure 4: Ecoregions across Oklahoma (EPA 2018)

3.2 Datasets

Oklahoma Mesonet

To calculate SPI and SPEI across the Chickasaw Nation (see section 3.3), this project utilized data from the Oklahoma Mesonet (hereafter "Mesonet") to ensure a higher spatial resolution than the climate-division scale drought indices that are currently available. The Mesonet is a network of 121 surface observing stations that measure environmental conditions every five minutes, and these stations are located across the 77 counties of state of Oklahoma (Brock et al. 1995; McPherson et al. 2007).

The data recorded at all stations are quality assured by both computer programs and human observations at the Oklahoma Climatological Survey (OCS) to ensure the data being reported to the user are free of significant errors (Fiebrich et al. 2006; Fiebrich et al. 2010).

The spatial resolution of ~30 km can support decision makers in many different sectors in the region (Shafer et al. 2000; Ziolkowska et al. 2017). Mesonet data have been used to examine county-scale meteorological phenomena across the state such as heatbursts (McPherson et al. 2011) and extreme weather events (Arndt et al. 2007). More specific to this study, data from the Mesonet have been used to analyze spatial characteristics of wet and dry periods through studies such as regional rainfall patterns (Boone et al. 2012) and soil moisture and drought (Illston and Basara 2003).

Within the 13 counties in the Chickasaw Nation, there are 19 Mesonet stations, with at least one in every county (Fig. 5). The data set includes daily precipitation (millimeters per day) and maximum and minimum daily temperature (degrees Celsius) for the usable length of record, 1998 - 2017. Due to an error discovered in the temperature measurements during the early stages of the Mesonet (1994-1997; Shafer et al. 2000), average daily temperature data before 1998 were not available for this study; thus our time series only includes the last 20 years of Mesonet data.

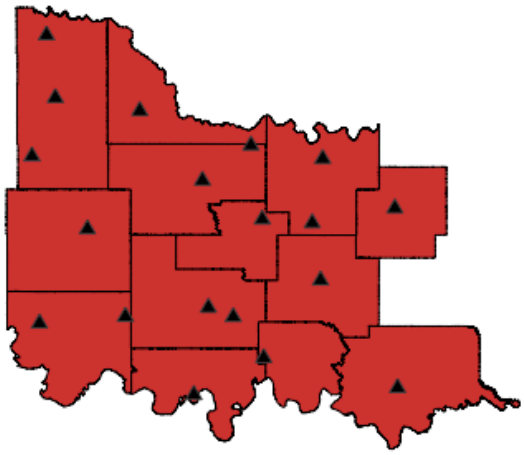

Figure 5: Locations of Oklahoma Mesonet stations across the Chickasaw Nation

U.S. Drought Monitor

The second main source of data was the U.S. Drought Monitor (USDM). Created by the National Oceanic and Atmospheric Administration, the U.S. Department of Agriculture, and the National Drought Mitigation Center, the USDM produces weekly maps depicting drought conditions, from D0 – Abnormally Dry to D4 Drought – Exceptional. The product is based on meteorological, hydrological, and soil moisture characteristics across the country. Furthermore, the Drought Monitor takes local user reports into account when creating their outputs (USDM 2018(a)), such as those available through the Drought Impacts Reporter (DIR 2018).

To best represent the monthly drought impacts using a weekly product for this study, we used the USDM map from the last week of each month to represent that particular month's drought conditions (USDM 2018(b)). This choice was made so that the USDM values reflecting the entire months climatic conditions were used in comparison to the SPI/SPEI products that were calculated using the entire months climatic conditions. There are several limitations of using the end-of-month USDM

product. First, these values only include conditions through the last Tuesday of each month, so any meteorological events (such as additional precipitation) from Wednesday until the last day of the month are not included in that month's USDM values. Second, during months when there was significant ramp up or decay of drought conditions, the single, end-of-the-month value may not be representative.

For every end-of-the-month USDM product in our time series, we extracted the USDM value at each Mesonet site by creating a function in RStudio (RStudio 2016) that rasterized the USDM's polygon shapefile data and extracted the value for each grid cell corresponding to the coordinates of each Mesonet station. These extracted values were merged into a single time series file for each Mesonet site.

For the purposes of this study, we define these extracted USDM values as the true condition of the drought (or "truth") at each Mesonet location. The USDM was selected as truth because it is a drought-monitoring tool that uses both objective and subjective variables, and its calculation relies on multiple sources of input (drought indices, hydrologic variables, expert input) in order to better monitor the impacts of drought across the region. A statistical comparison of our SPI and SPEI values to USDM values gives insight to how well our calculated indices represent drought conditions (see section 3.4 below).

Hydrologic Data

We chose to investigate drought impacts across the Chickasaw Nation based on the conditions of the hydrologic variables because of the importance of the hydrologic resources on the Nation and its people. To better understand how drought influences the hydrologic resources from community to community, it was necessary to evaluate the

physical effect on hydrologic variables during an extended period of drought. While there are many types of hydrologic variables (see section 2.4), we focused the scope of this study on discharge from rivers, streams, and springs. River, stream, and spring discharge (cubic feet per second) data were obtained through the United States Geological Survey's (USGS) National Water Information System (USGS 2018), and a time series was created from the available dataset for each hydrologic data site. The periods of record available for discharge data were not consistent nor complete across the same period as that of our drought indices, so we elected to take a subset of the data to evaluate a single drought event that impacted the region — the 2011 - 2015 drought.

Observing sites were only used in this study if they were within the bounds of the Chickasaw Nation and if they had a complete time series from 2011 – 2015, resulting in a dataset for one spring and 12 rivers and streams throughout the Chickasaw Nation. These gauges were more centrally located in the study as compared to the Mesonet stations due to the nature of the hydrologic resources across the region — that is, the majority of rivers, streams, and springs are clustered around the Arbuckle-Simpson Aquifer.

Using the WaterData package in RStudio (Ryberg and Vecchia 2012), the hydrologic data were evaluated to ensure there were no large gaps of missing values (less than 30 days), and any missing values were filled and smoothed using the *fillMiss* function within the WaterData package (Ryberg and Vecchia 2012) that utilizes a state-space model for fixed-interval smoothing on the time series. Of the 13 stations, only three had missing values over their period of record, with a maximum of 0.04% of data missing from any single station. Smoothing of the dataset was done to ensure each

station had a continuous time series, which was essential for the statistical evaluation of the data (see section 3.4).

3.3 Derived Products

With this study's aim to better analyze the localized drought severity and spatial variability of drought across our domain, we derived a dataset of SPI and SPEI from the Oklahoma Mesonet data that has a spatial resolution appropriate for this study region. To do this, we utilized the *SPEI* package in RStudio (Beguería and Vicente-Serrano 2013) to compute time series for both indices across Chickasaw Nation as a whole and for each of the 19 Mesonet stations. The calculation for SPI only requires daily precipitation data while the calculation for SPEI uses the difference between precipitation and evapotranspiration, the latter of which is estimated using average daily temperature, latitude, and the Thornthwaite equation (Thornthwaite 1948). To standardize the data, RStudio's *SPEI* package uses a gamma distribution for SPI and a log-logistic distribution for SPEI. Figure 6 is an example of time series plots of SPI and SPEI on 1-, 3-, and 12-month time scales for one station within the Chickasaw Nation (Sulphur, OK):

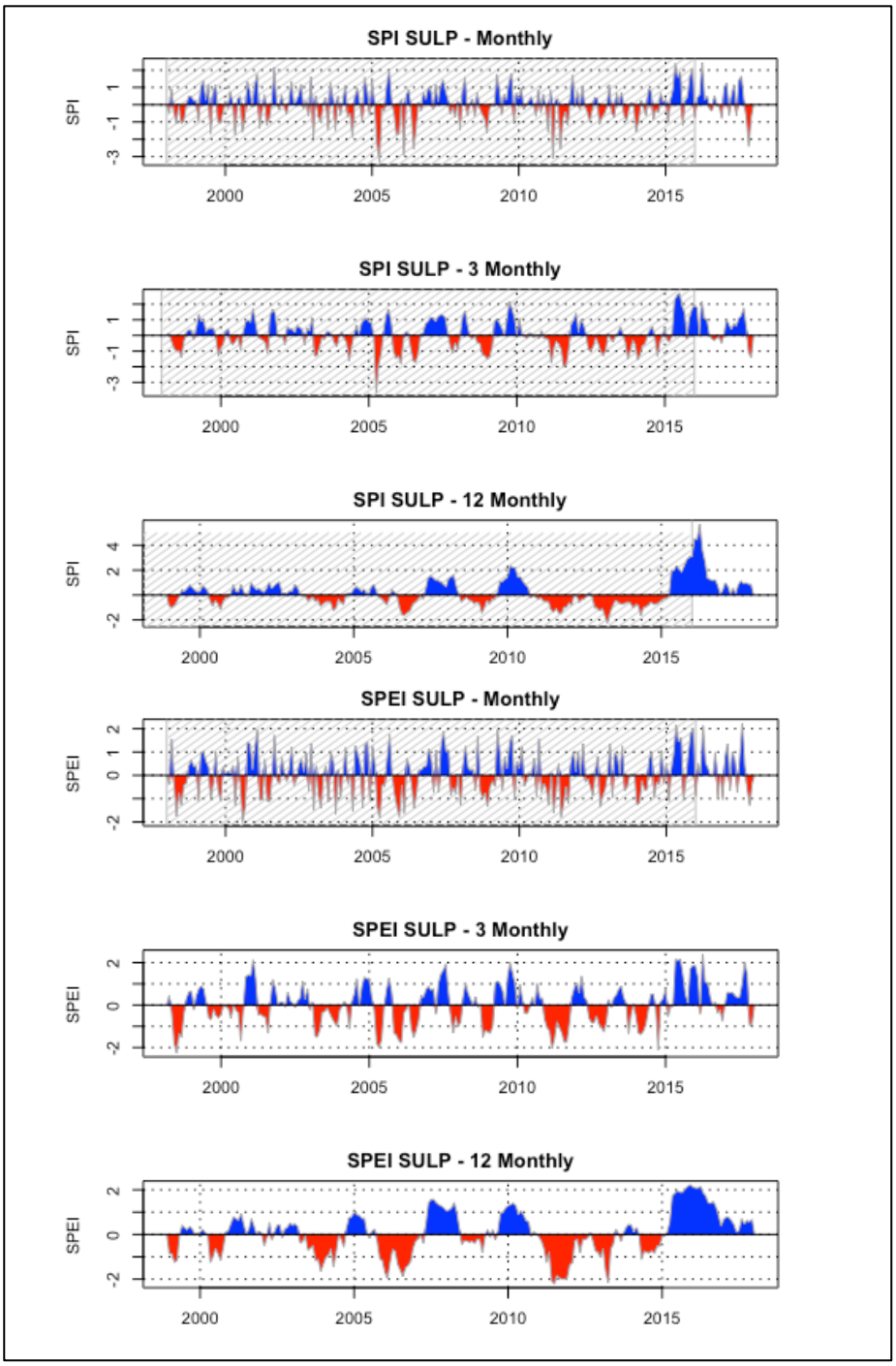

Figure 6: Time series of SPI and SPEI on 1-, 3-, and 12-month time scales at the SULP Mesonet station located in Sulphur, Oklahoma.

To visualize the spatial variations in the data, we created maps of each index for all months in the period of record. For this, we utilized inverse-distance weighted

(IDW) interpolation (Brunsdon and Comber 2015) through the default function in the *gstat* package in RStudio (Pebesma 2003), with no variogram or linear model (due to the lack of relationship between the locations of Mesonet stations). IDW interpolation assumes that variables at stations closer together are more related than those at stations farther apart and assigns grid cells a weighted average value that decreases as distance increases. This interpolation method was performed across our domain, and the resulting output was mapped to mimic the USDM color scheme to better visualize how SPI and SPEI varied from our selected "truth" dataset.

To better understand if drought indices calculated on a climate division scale are representative of the localized drought severity in that region, it was necessary to compare our dataset to a single calculation of drought representing the entire region. We justified characterizing the data over the Chickasaw Nation as climate division-scale data due to its comparable spatial extent to a climate division. Climate division 8 (CD8) in south-central Oklahoma is the closest climate division to our study area, and the bounds only differ by three counties (Atoka county is included in CD8, and McClain and Grady counties are not) and five Mesonet stations (Lane is included in CD8 and Minco, Chickasha, Acme, and Washington are not). Therefore we considered our study area to be representative of a climate division. First we calculated a single SPI and SPEI value for the entire Chickasaw Nation over the same period of record. This dataset was analyzed in the same method as the station-based dataset (see section 3.4).

3.4 Analysis Method

To perform a proper qualitative analysis of the spatial and seasonal patterns observed in the interpolated maps of SPI and SPEI, we first had to define drought

conditions. McKee et al. (1993) defines drought as any extended period where the SPI reaches a value less than or equal to -1.0. Any drought event is characterized by the duration and frequency of the period of drought, with short-term droughts (time scales of 1 to 3-months) and long-term droughts (12-months or more) (McKee et al. 1993). In addition, rapid development (decay) in drought is when SPI values quickly change from wet (dry) to dry (wet) over the corresponding time scale (i.e. from month-to-month in 1-month SPI or over three months in 3-month SPI). We will use these definitions through the remainder of the analysis.

We performed significance testing on our derived SPI and SPEI datasets to assess the differences in the populations of indices. First, we calculated the mean and standard deviation (sd) of the data to investigate the variability of the datasets. We then conducted a nonparametric test of significant differences using the Mann-Whitney-Wilcoxon test, which does not require the samples to be of a normal distribution. This was performed using the Wilcoxon two-sample test function in the "stats" package supported in RStudio (RStudio 2016).

Root Mean Square Error

We analyzed the quality of our derived data by testing the SPI and SPEI values against those for the U.S. Drought Monitor for each month from 2000 to 2017. We utilized the root-mean-square error (RMSE; Equation 3.1; Wilks 1995) calculated using two datasets over the same set of points as follows:

$$RMSE = \sqrt{\frac{1}{M}\sum_{m=1}^{M}(y_m - o_m)^2} \qquad \text{(Equation 3.1)}$$

where M is the total number of evaluated grid points, y_m is the calculated value for each gridpoint m, and o_m is the observed value at each gridpoint (i.e., the value of the USDM

at that gridpoint). RMSE is a method of measuring the accuracy of a calculated variable against the observed values for that field; as the RMSE increases, the accuracy of the calculated value decreases (Wilks 1995). One advantage of using RMSE rather than the mean square error (MSE) is that RMSE preserves the units of the variable, which is useful for a categorical variable like USDM (Wilks 1995).

Prior to calculating the RMSE values, we defined a difference of two USDM categories (e.g., D0 vs. D2, D1 vs. D3) as a "substantial error." For these calculations, the values of SPI and SPEI were transformed to reflect the USDM categories (Table 4), as defined in Svoboda et al. (2002). The transformed SPI/SPEI datasets and the respective USDM dataset were adjusted by a value of +1 (e.g., USDM D4 drought was assigned a value of 5) to assign periods of no drought with a value of 0 (Table 5), ensuring no negative values.

Table 4: U.S. Drought Monitor category and description with the assigned SPI range for each category (Svoboda et al. 2002)

USDM Category	USDM Description	SPI Range
D0	Abnormally dry	-0.5 to -0.7
D1	Moderate drought	-0.8 to -1.2
D2	Severe drought	-1.3 to -1.5
D3	Extreme drought	-1.6 to -1.9
D4	Exceptional drought	≤ -2.0

Table 5: U.S. Drought Monitor category and description with the assigned SPI range for each category (Svoboda et al. 2002)

Original USDM Category	USDM Description	Adjusted value for USDM and SPI/SPEI
NA	No Drought	0
D0	Abnormally dry	1
D1	Moderate drought	2
D2	Severe drought	3
D3	Extreme drought	4
D4	Exceptional drought	5

To further understand if these data, calculated on a climate division scale, were representative of the localized impacts in that region, we created a new dataset using spatially weighted average values for each time scale of SPI and SPEI over the Chickasaw Nation as a whole. The weightings of each of the 19 stations were computed using Thiessen polygons using the *delidir* package in RStudio (Turner 2007) over the boundary of the Chickasaw Nation, and weighted averages of SPI and SPEI values were calculated for each month in the period of record. Spatially weighted values were used to account for any clustering of the Mesonet stations, though we found minimal clustering and, thus, little difference between the spatially weighted averages and the simple computed means. These datasets were then analyzed using the same method as the station SPI/SPEI data, with one value representing a climate-division value for each month.

Hydrologic Analysis

To answer our final research question (i.e., the spatial variation of drought impacts on hydrologic resources), we conducted a case study of the 2011 – 2015 drought to better understand how surface water resources within the Chickasaw Nation

were impacted during a multi-year drought. We first calculated normal monthly streamflow by averaging the streamflow for each individual month over the historical period for each station. Assuming all streams in the dataset were perennial, the 12 monthly values (January through December) were then used to calculate the percentage of normal streamflow for each station from 2011 to 2015 using equation 3.2:

$$PNS = \frac{(s_m - \bar{s}_m)}{\bar{s}_m} \times 100 \qquad \text{(Equation 3.2)}$$

where s_m is the streamflow and $\bar{s}_m$ is the normal streamflow for that respective month, m. Next, each USGS streamflow measurement station was paired with its nearest-neighbor Mesonet station to approximate their respective SPI and SPEI values. These stations were paired under the requirements that: 1) the Mesonet station was located upstream from the USGS station and 2) the station was within the same drainage basin. It was important to identify a drainage basin of appropriate scale for this analysis. While hydrologic unit code (HUC) 12 provides a more detailed depiction of the runoff region for each stream and its tributaries, only three of the USGS observing stations (Antelope Springs, Little Washita, and Pennington Creek) meet both of these conditions (Fig.7). Because of this, we had to use the HUC 8 drainage basins to pair the remaining USGS and Mesonet stations that are located within the same basins (Fig. 8).

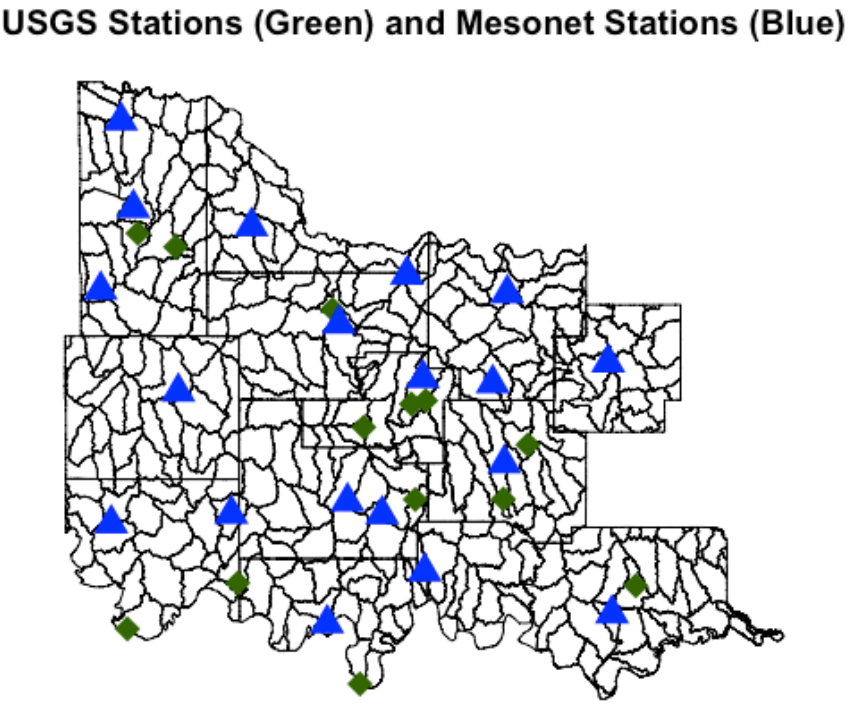

Figure 7: USGS stations (green) and Mesonet Stations (blue) over the HUC-12 drainage basins (thick black) across the Chickasaw Nation.

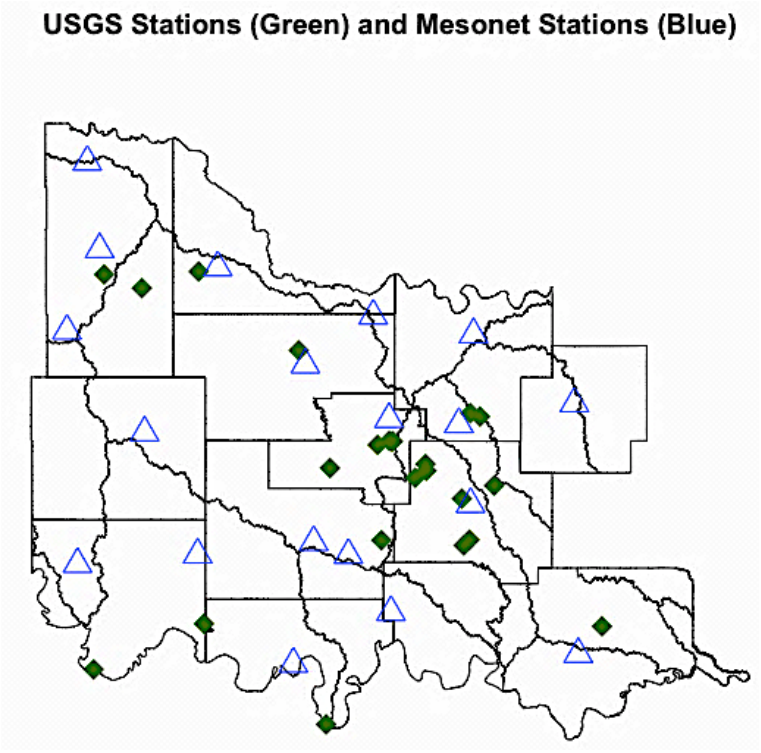

Figure 8: USGS stations (green) and Mesonet Stations (blue) over the HUC 8 drainage basins (thick black) across the Chickasaw Nation.

Due to these constraints, a traditional nearest-neighbor distance calculation for the points was not appropriate, so the nearest neighbor was selected manually. The time series analysis used a cross-correlogram from 1- to 6-month lags with the 1-, 3-, and 12-month SPI and SPEI products. The cross-correlograms display the temporal cross-correlations between SPI (or SPEI) and percentage of normal streamflow, and allow the user to observe any lagged interactions between the different datasets. In addition, cross-correlograms allow us to better determine if there is a direct or indirect relationship between the two variables, and view if there are any secular patterns, or patterns that are consistent over time rather than seasonal or periodic trends.

Chapter 4: Results

To examine the spatial variation of drought and its impacts on the Chickasaw Nation, we ask the following questions:

- Is the drought severity within the boundaries of the Chickasaw Nation better represented with SPI or SPEI on one-, three-, or 12-month scales? Is there a spatial or seasonal component to the differences in how these indices represent drought severity?
- Are SPI and SPEI calculated on a climate-division scale representative of the localized impacts in the study region?
- How does drought impact the hydrologic resources from community to community across this study region?

4.1 Statistical Evaluation of SPI/SPEI

To begin answering the first of these questions, we evaluated whether SPI and SPEI on the three different time scales represented different populations. First we applied the Mann-Whitney-Wilcoxon test (section 3.4) for SPI and SPEI on 1-, 3-, and 12-month scales. Although the variability of SPI 1-month (standard deviation, SD = 0.98) was larger than SPEI 1-month (SD = 0.95), the difference was not statistically significant (p = 0.29). Similarly, the variability in 3-month calculations of SPI (SD = 0.96) and SPEI (SD = 0.96) were not significant (p = 0.14). Finally, while the variability of the SPI 12- month (SD =0.98) calculations was slightly larger than that of the SPEI 12-month (SD = 0.97), they also were not statistically significant (p = 0.83). From these numbers, we conclude that the difference between the SPI and SPEI datasets for all time intervals was not statistically significant. Because there is not a statistically significant

difference in the means of the SPI and SPEI datasets, we know that they do not represent drought differently across the Chickasaw Nation.

Seasonally, we found significant differences between SPI and SPEI in the winter (December, January, and February) and spring (March, April, May) 12-month calculations ($p = 0.008$and $p = 0.017$, respectively). This result in significance testing indicates that there is a difference between the means of the two data sets when partitioned by these respective seasons. We resolve that the seasonal datasets of SPI and SPEI are in fact representing drought differently during those time frames because there is a statistically significant difference between the populations during the winter and spring 12-month time scales.

To justify using SPI and SPEI values, we compared these calculated indices to the U.S. Drought Monitor (which we earlier defined as "truth"). The average RMSE error was computed using SPI/SPEI and USDM values adjusted to avoid negative values. Because a 0.1 difference in SPI or SPEI value could result in it being associated with one drought-monitor category difference, we defined a "substantial error" in the SPI or SPEI values as any RMSE greater than or equal to 2.0 — a two-category difference from the USDM value. Table 6 itemizes the individual errors for each SPI and SPEI dataset. The errors in SPI are lowest during the 12-month time scale, yet the errors in SPEI do not vary much between the time scales.

Table 6: Root Mean Squared Error (RMSE) for the station SPI and SPEI time series on 1-, 3-, and 12-month time scales.

Time Scale	SPI	SPEI
1-month	1.8	1.7
3-month	1.6	1.6
12-month	1.5	1.7

Following the analysis of the SPI and SPEI datasets as a whole, we investigated if the error in monthly SPI/SPEI varied by season over the time period. From our monthly RMSE for each time scale, we averaged those values for winter (DJF), spring (MAM), summer (JJA), and fall (SON). Looking seasonally, the errors were lowest during the spring for all time scales (Table 7). SPI 3-month spring had the lowest RMSE of any seasonal calculation with 1.1. The season with the highest average RMSE was fall, at 1.4. Spring had the lowest RMSE of all the seasons, but overall the variances between seasons were small with a maximum difference of 0.2. This signifies that there is less of a difference between our calculated datasets when we compare these values seasonally.

Table 7: Seasonal Root Mean Squared Errors (RMSE) for SPI and SPEI on 1-, 3-, and 12-month time scales

Season	SPI	SPI 3-Month	SPI 12-Month	SPEI	SPEI 3-Month	SPEI 12-Month
Winter	1.4	1.2	1.2	1.3	1.2	1.4
Spring	1.3	1.1	1.1	1.2	1.2	1.3
Summer	1.3	1.2	1.2	1.2	1.2	1.4
Fall	1.5	1.4	1.2	1.4	1.4	1.4

Looking at the RMSE values calculated over each month in the period of record for the six time series, every product had at least one month with an error greater than

4.0, with SPI and SPEI 1-month having the largest RMSE of 4.69 and 4.86, respectively. These datasets also had the largest number of months with RMSE greater than or equal to 4.0 (6 and 7 months, respectively). Figure 9 displays the distribution of RMSE values for each monthly dataset. SPEI 3-month and SPI 12 month had the greatest percentages of months with RMSE below 2.0 (81.9% and 81.0%, respectively). SPI 12-month and SPEI 1-month had the largest number of months with no error (RMSE = 0.0) for 34 months, or 15.7%. The product with the largest percentage of months above the threshold was SPI 1-month — 57 months with RMSE greater than 2.0.

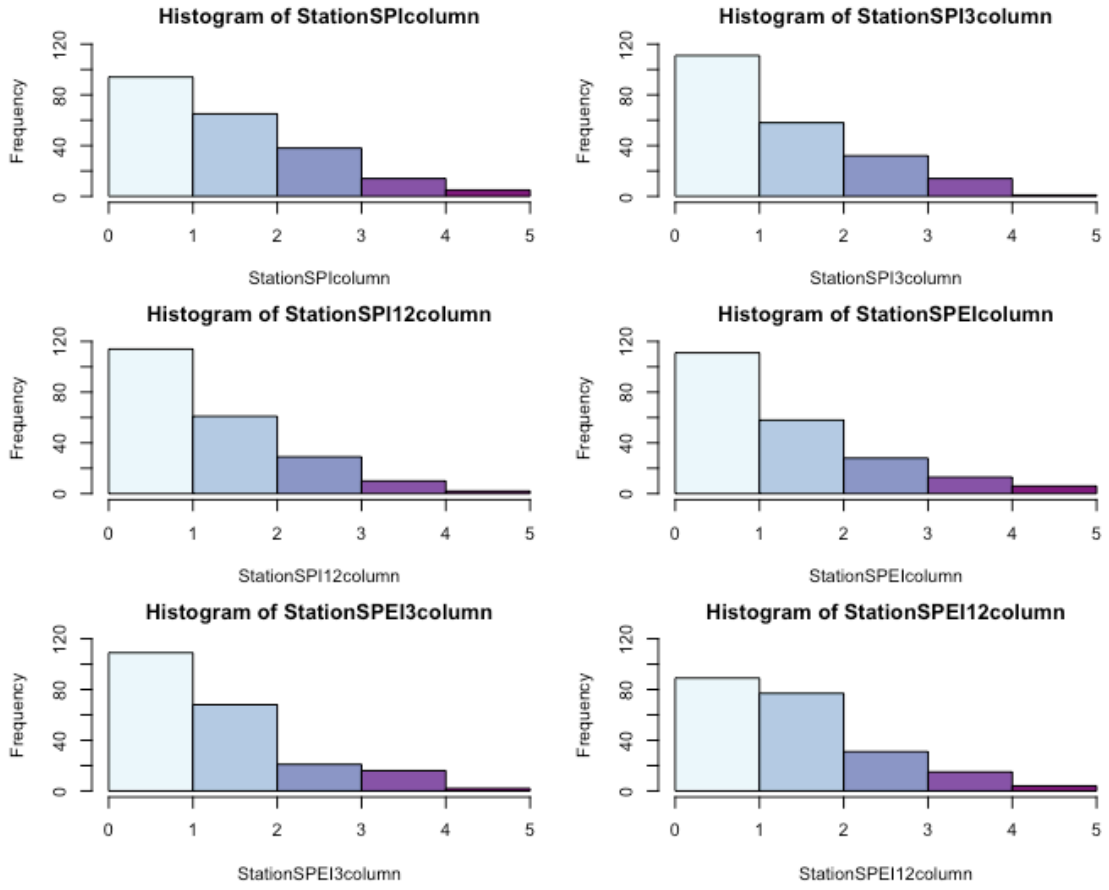

Figure 9: Distribution of RMSE values for the monthly datasets of SPI and SPEI for 1-, 3-, and 12-month time scales

We examined how the RMSEs varied spatially across the study area, finding that the RMSE is higher for our station-based results (Table 8). The highest (lowest) RMSE was 2.1 (1.2) at the Ardmore (Centrahoma) Mesonet site for the SPEI (SPI) 12-month product Four stations had substantial errors above the two-category threshold: Ardmore (SPEI 12-month), Waurika (SPI 1-month & SPEI 1-month), and Madill (SPEI 12-month). To investigate the distribution of errors further, we plotted the spatial extent of these values over the Nation. Looking spatially across all SPI and SPEI products, the errors were largest (smallest) in the counties in the southwest (northeast) corner of the region, as seen in Figure 10.

Table 8: Root Mean Squared Error (RMSE) for each Mesonet Station in the Chickasaw Nation over 1-, 3-, and 12-, month time scales

Station	SPI RMSE	SPI3 RMSE	SPI12 RMSE	SPEI RMSE	SPEI3 RMSE	SPEI12 RMSE
ACME	1.9	1.7	1.5	1.9	1.6	1.7
ADAX	1.7	1.4	1.4	1.6	1.4	1.5
ARD2	1.8	1.8	1.8	1.7	1.8	2.1
BURN	1.7	1.5	1.6	1.7	1.5	1.6
BYAR	1.7	1.5	1.3	1.6	1.5	1.7
CENT	1.6	1.4	1.5	1.6	1.4	1.5
CHIC	1.7	1.5	1.4	1.6	1.5	1.6
DURA	1.8	1.5	1.5	1.7	1.6	1.7
FITT	1.7	1.7	1.7	1.6	1.9	1.7
KETC	1.9	1.7	1.5	1.8	1.9	2.0
MADI	1.8	1.6	1.4	1.7	1.5	1.6
MINC	1.7	1.5	1.5	1.6	1.5	1.5
NEWP	1.8	1.8	1.9	1.7	1.9	2.0
PAUL	1.7	1.5	1.3	1.7	1.5	1.7
RING	1.9	1.7	1.6	1.8	1.6	1.8
SULP	1.7	1.5	1.4	1.7	1.5	1.6
TISH	1.7	1.5	1.4	1.6	1.5	1.6
WASH	1.7	1.5	1.4	1.7	1.5	1.6
WAUR	2.1	1.8	1.7	2.1	1.8	2.0

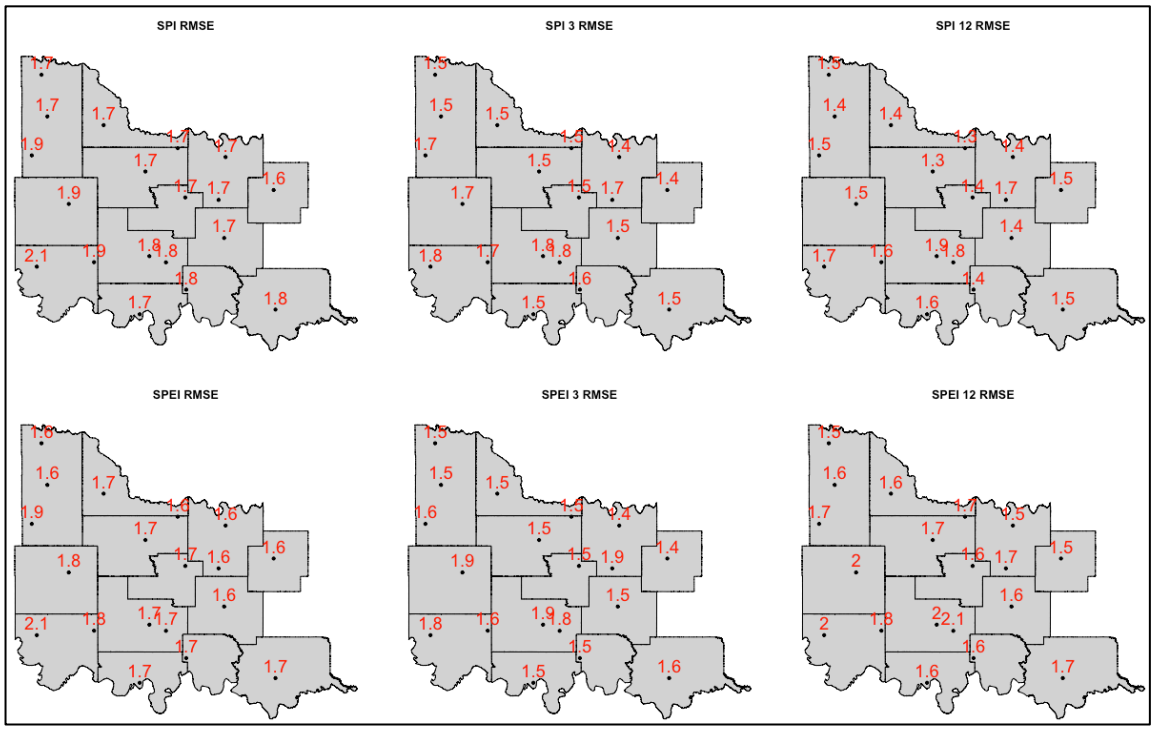

Figure 10: Root Mean Squared Error (RMSE) over the Chickasaw Nation for individual station SPI (top) and SPEI (bottom) on 1- (left), 3- (center), and 12-month (right) time scales

One interesting result was that the only months with a RMSE of zero were months that both the SPI/SPEI value and the USDM value were equal to zero; that is, there was no drought throughout the region. Looking more closely at the original datasets, many of these months had positive SPI/SPEI values, and all of the occurrences of RMSE equal to zero had USDM maps with no drought (or NA values from the extracted dataset).

These extreme errors (RMSE > 4) were observed in the SPI (SPEI) products for 6 (7) months in the 1-month dataset, 1 (2) months in the 3-month dataset, and 2(4) months in 12-month dataset. In addition, all of the extreme errors occurred during months of persisting drought, with 26% (30%) of those months in the 1-month dataset, 4.3% (8.7%) in the 3-month dataset, and 8.7% (17%) in the 12-month dataset. Looking

more closely at the RMSE values during drought events, we see more errors above our threshold in the 1-month datasets of SPI and SPEI. For example, during the 2011-2015 drought, there were 23 months, or 38% of the 5-year period, in the SPEI 1-month data set with a substantial error of RMSE above the threshold of 2. Overall, the 1-month datasets of SPI and SPEI had the largest errors when calculating RMSE by individual month.

It should be noted that there might be some biases in the error calculations that should be considered. Examining the calculate RMSE values found that all instances of RMSE equal to zero were during times when both USDM and the transformed dataset of SPI/SPEI were depicting a month with no drought conditions, or both values were equal to zero. These instances may provide a lower bias to our overall RMSE values for each dataset. If we removed all months with RMSE and the transformed dataset of SPI/SPEI equal to zero, almost certainly we would see larger errors for all datasets.

4.2. Spatial, temporal, and seasonal variability of SPI and SPEI

Continuing with our first question, we wanted to investigate if drought severity was better represented by the 1-, 3-, or 12-month SPI and SPEI products. To do this, we first looked at the distributions of our original SPI/SPEI datasets across these time scales. Figure 11 displays boxplots that represent the variability of SPI and SPEI at each Mesonet station for the three time scales. First, these graphics reveal that the majority of stations have median values at or near zero, as is expected with the standardization of the precipitation values in calculating these indices. Comparing the distribution of SPI and SPEI across the stations, we can see that across a majority of the stations, the range is evenly distributed, but there is clearly more variability in the ranges for the boxplots

of the three SPI datasets. In particular, there are far more outliers in the SPI datasets as compared to the SPEI datasets, with many negative outliers in the SPI 1- and 3-month datasets and considerably more positive outliers in the SPI 12-month dataset. The large number of outliers in these datasets signifies that there is more variability outside the upper and lower quartiles for SPI than for SPEI. We know the average standard deviation for all time scales of SPI (SD = 0.97) is slightly larger than that of SPEI (SD = 0.96), and using this information and their boxplots, it is understood that SPI products have slightly more variability across all of the stations.

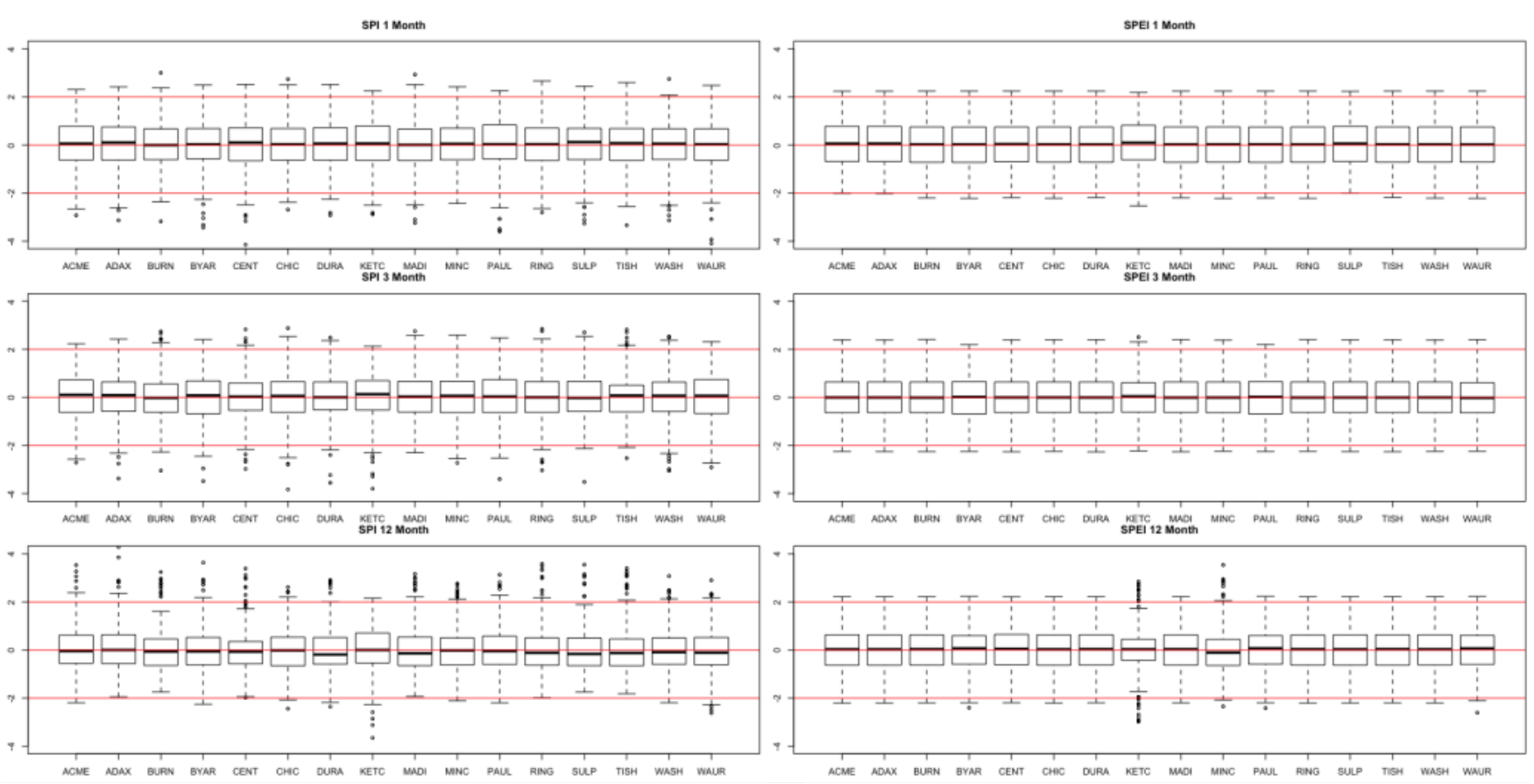

Figure 11: Boxplots for SPI (left) and SPEI (right) on 1-(top), 3-(middle), and 12-month (bottom) time scales

The larger variability in the first and fourth quartiles of the SPI datasets is consistent with the RMSE calculations. These SPI outliers were found to have occurred during extended periods of drought, including the 2005-2006 drought and 2011-2015 drought. A closer look at the variability in the SPI 1-month dataset, we found that out of the 22 months in that dataset that had a value less than -3, 11 of those months were during 2011 and six of those months were during the 2005-2006 drought.

Following the analysis of the distribution of each dataset, we continued our investigation of the 1-, 3-, and 12-month time series and their representation of drought severity across the region. First we examined the spatial variability of drought severity across the three time scales for the SPI and SPEI datasets that were calculated for each Mesonet station, looking for any distinct patterns across the indices. We first performed a qualitative assessment of the month-to-month variations in values using interpolated maps over the study area. The symbology of the maps was characterized such that original values of SPI and SPEI would visually represent the USDM categories, as in Table 4. Using these maps, we identified patterns in the development of drought, short-term and long-term manifestation of drought, and the occurrence of different magnitudes of drought.

There were two main drought events that occurred during the period of record: the 2005 – 2006 and the 2011 – 2015 droughts. The other instances of drought were short lived. As the literature suggested (Mckee et al. 1993; Vicente-Serrano et al. 2010), maps of SPI and SPEI interpolated across the stations for 1- and 3-month time scales depicted more frequent droughts with shorter durations, and the 12-month time scale had less frequent droughts with longer durations. The SPI 1-month station dataset had

98 months (40.8%) with at least one station less than or equal to -1, and the SPI 12-month station dataset had 84 (36.7%). On the contrary, the SPEI datasets for the same time scale did not exhibit these same patterns, as the 1-month calculations had the lowest number of drought occurrences with 42 (17.5%) and the 3-month calculations actually had the most months with an occurrence of drought with 61 (25.7%) months, with the 12-month totaling just below the 3-month with 58 (25.3%). Another notable finding from the drought frequency analysis is that SPEI had far fewer months with drought occurrence than SPI for all time scales, but those months where the SPEI datasets did depict drought had more stations with drought conditions than SPI. This indicates that SPEI depicts less frequent drought, but droughts with more spatial coverage across the region.

Compared to SPEI, SPI displays more rapid, localized development of drought across the region. While SPEI also exhibits periods of rapid development, it is more evenly distributed across the region. Figure 12 shows a visual example of how the values of SPI and SPEI develop across the region during a time scale that was found to have statistically significant differences between the SPI and SPEI datasets (1-month spring). While both maps of SPI and SPEI 1-month values indicate that the area is under the same magnitude of drought, D3 – extreme drought, in the far right maps (March 1998), the map for SPEI 1-month indicates that the entire area us under extreme drought while SPI 1-month emphasizes two distinct areas of extreme drought with the majority of the region under D2 severe drought. The variability in values can be captured quantitatively in the standard deviations for each time period. The standard deviations for SPEI 1-month during March, April, and May 1998 (SD = 0.026, 0.048, 0.022,

respectively) are one order of magnitude smaller than those of SPI (*SD* = 0.21, 0.75, 0.37, respectively). Furthermore, the average difference in SPEI 1-month values from month-to-month was larger than that of SPI 1-month. This rapid development is consistent with the overall change from March to May 1998, with 3.40 increase in drought for SPEI 1-month and 2.79 for SPI 1-month. The results from this example are consistent with the average difference of SPI (SPEI) values from month-to-month for all three time series with 1-, 3-, and 12-month difference equal to 0.95 (1.10), 0.52 (0.57), and 0.26 (0.29), respectively.

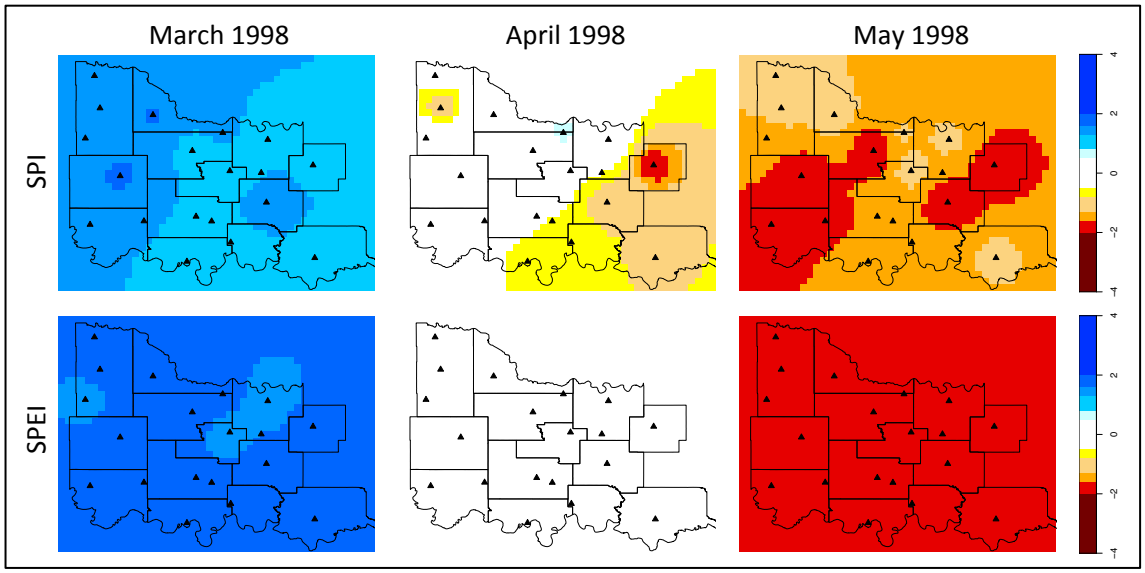

Figure 12: Values of SPI (top row) and SPEI (bottom row) across the 13 counties of the Chickasaw Nation for March 1998 (left column), April 1998 (center column), and May 1998 (right column). Values in cool colors (e.g., blue) represent wetter periods; values in warmer colors (e.g., orange) represent drier periods.

After looking at the variations in SPI and SPEI across the 1-month time scale, we continue with our examination of which time series of SPI and SPEI represents drought severity the best by comparing the localized differences across the three time scales: 1-month, 3-month, and 12-month. Looking these instances of the progression of

drought over the three time scales, the average month-to-month difference of the station values of SPI (SPEI) are 0.95 (1.06) for 1-month, 0.52 (0.57) 3-month, and 0.26 (0.29) 12-month. Not only is the average month-to-month difference slightly larger in all three SPEI time scales, the SPEI 1-month difference is largest of the six datasets. These results are consistent with our calculated values for this example. Visually, the dissimilarities across time scales are seen to have "hot spots" — areas on the map with increased/decreased magnitudes of drought relative to the adjacent grid boxes — that are reflected across time scale maps during that particular month. The variability is observed during both periods of drought (continuous values of SPI/SPEI < -1) and during periods of excess moisture (continuous values of SPI/SPEI > 1) (Agnew 2000; Guttman 1999; McKee et al. 1993).

Examples of these results are highlighted in maps showing a period of long-term drought September 2011 (Fig.13) and a period of no drought May 2007 (Fig. 14). Visually, SPEI maps portray a more uniform field, with fewer, if any, hot spots while the SPI maps have many hot spots. Using this example of variability across the three time scales during times of drought, we calculated the standard deviations for each product. For the month representing drought conditions (September 2011) the SPI and SPEI 1-month products have the lowest standard deviations of the three time scales (0.42 and 0.03, respectively), with 3-month (0.61 and 0.11, respectively) and 12-month (0.55 and 0.21, respectively) calculations having similar results. The results for the variations in SPI and SPEI values for the month representing wet conditions (May 2007) show much less variation in SPEI with standard deviations for SPI (1-month: 0.37, 3-month: 0.49, 12-month: 0.62) being one order of magnitude larger that those of

SPEI (1-month: 0.002, 3-month: 0.014, 12-month: 0.070), and they are lowest for both SPI and SPEI 1-month. From these maps, we determined there is less spatial variability in SPEI, which can be attributed to the influence of a relatively uniform temperature gradient across the small region.

Both SPI and SPEI exhibit variability between the 1-, 3-, and 12-month calculations, and the standard deviations also confirm that the spatial variations in SPEI are lower than SPI for all time scales, preserved over both dry and wet conditions, with an average standard deviation for SPEI of 0.12 (dry) and 0.071 (wet) as compared to 0.52 (dry) and 0.49 (wet) for SPI.

The 1-month calculations for both SPI and SPEI contain drastic changes month-to-month, evolving from exceptional drought to no drought in the matter of two to three months; this observation is reflected in the standard deviation values. These observations are confirmed when looking at the different boxplots in Figure 11. The SPI 1-month plot has the largest spread between upper and lower quartiles and the smallest spread between the quartiles in the 12-month calculation, but the SPEI quartiles stay more consistent across the three time scales. SPI has more temporal variability, but both indices portray this variability across the different time scales. In addition, the short-term times scales are responsive to monthly increases and decreases in precipitation, leading to the rapid intensification or reduction in drought severity.

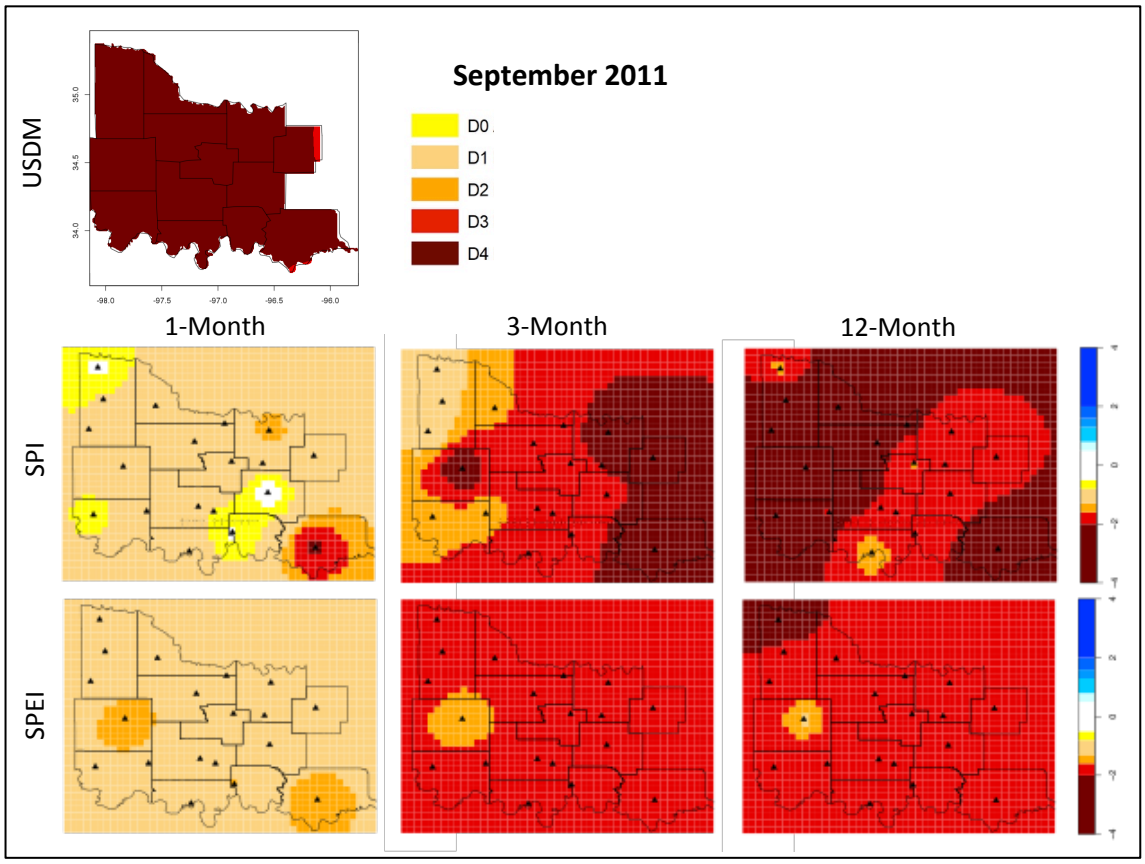

Figure 13: One-month (left), 3-month (center), and 12-month (right) values for SPI (top) and SPEI (bottom) across the Chickasaw Nation for the month of September 2011.

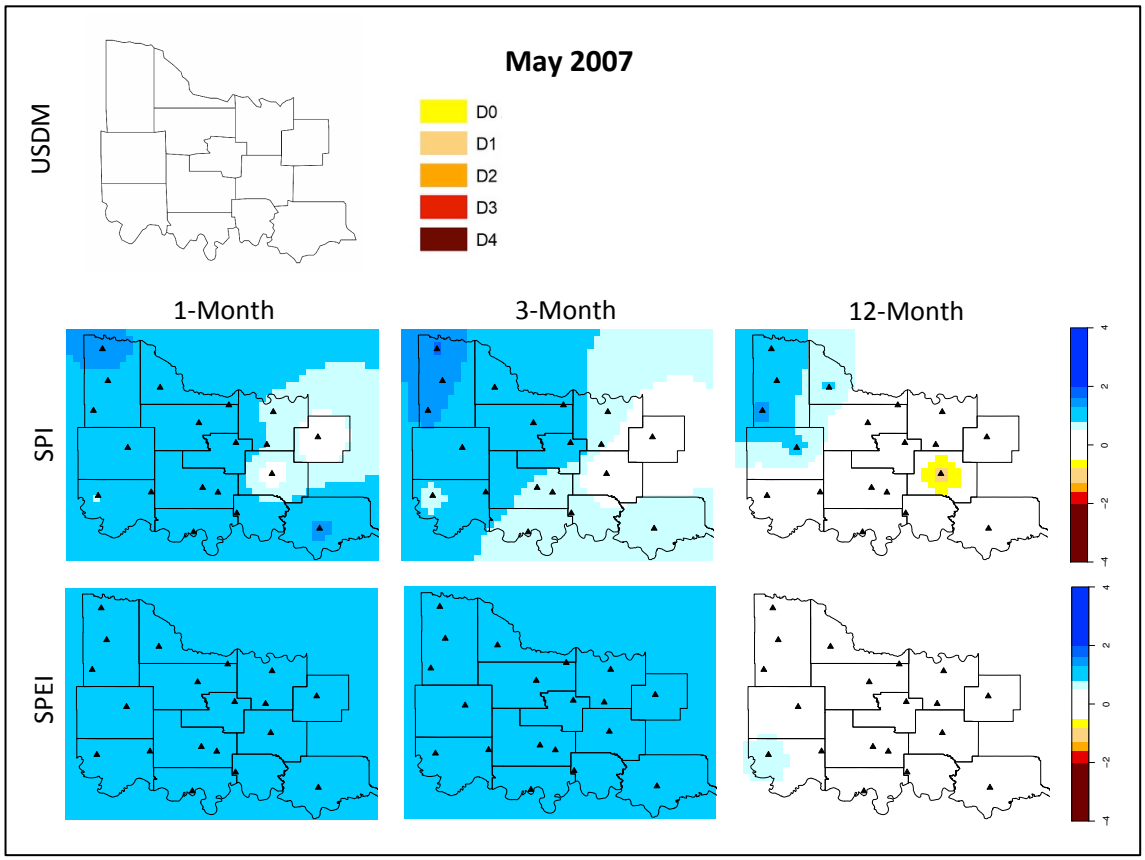

Figure 14: Same as Figure 13 except for the respective period ending in May 2007

Combining the concepts of spatial variability and variability across product time scales, we investigated how the SPI and SPEI datasets represented drought seasonally across the Chickasaw Nation. Wet seasons had a clear impact on 1-month SPI/SPEI values, and 3-month SPI/SPEI plots presented seasonal patterns as this time frame incorporated the conditions over the entire season. Plots of the 12-month products are less influenced by seasonal variances, as they portray the long-term patterns better than the other products.

Two crucial examples for this analysis depicting seasonal differences between the two indices are seen when comparing times of persisting drought over a warm season (Summer 2011; Fig. 15) and a cool season (winter 2005/2006; Fig. 16). We can

see many temporal and spatial differences across both seasons. The spatial continuity of SPEI is retained across all seasons, with the higher magnitude of drought in SPEI maps during the summer months, or times of higher temperatures (Fig. 15). During winter months there is slightly less variability between the SPI and SPEI calculations due to less influence of evapotranspiration (Fig. 16). The variability of SPI month-to-month was larger than that of SPEI for both winter and summer, and in fact, the variability of SPI (*SD* = 1.2, 0.77, and 0.56 summer, 0.93, 0.56, 0.43 for 1-, 3-, and 12-month winter, respectively) over both seasons was larger than that of SPEI (*SD* = 0.57, 0.32, 0.33 summer, 0,60, 0.18, 0.37 for 1-, 3-, and 12-month winter, respectively).

Another noticeable pattern in the maps of SPI and SPEI is that the SPEI 12-month maps depict a more severe drought magnitude as compared to the SPI 12-month maps. There is a visible increase in variability in the 3 and 12-month calculations due to influence of the longer-term trends in the dataset. To confirm this hypothesis, we calculated the mean values of SPI and SPEI across all of the stations for the entire season, verifying that indeed the mean of the SPEI plots (-1.92) was larger than that of the SPI plots (-1.50). This analysis was repeated for the winter months; while the difference was not as large as the summer months, the mean of the SPEI plots (-1.52) was larger than that of the SPI plots (-1.16) over the winter months as well. This time scale allows the user to view the long-term patterns of drought in the region.

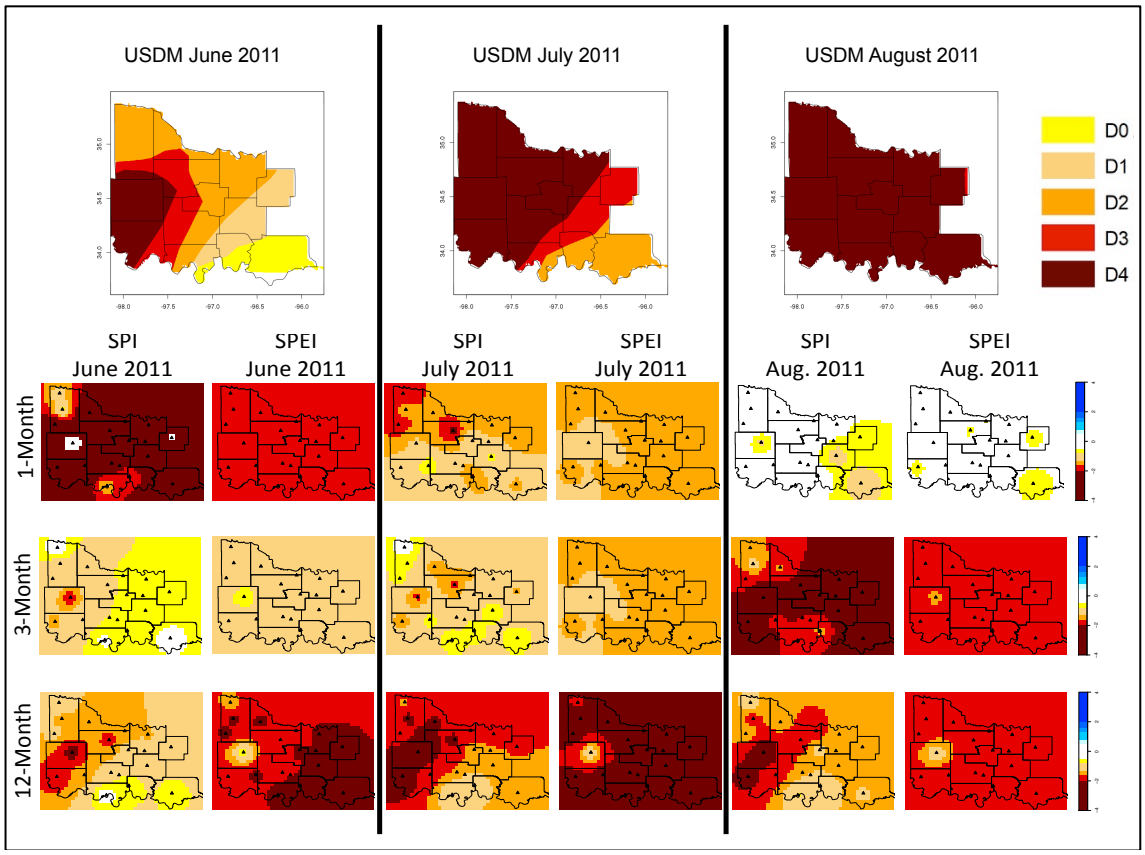

Figure 15: SPI/SPEI over the Chickasaw Nation for June, July, and August 2011 on 1-, 3-, and 12-month time scales

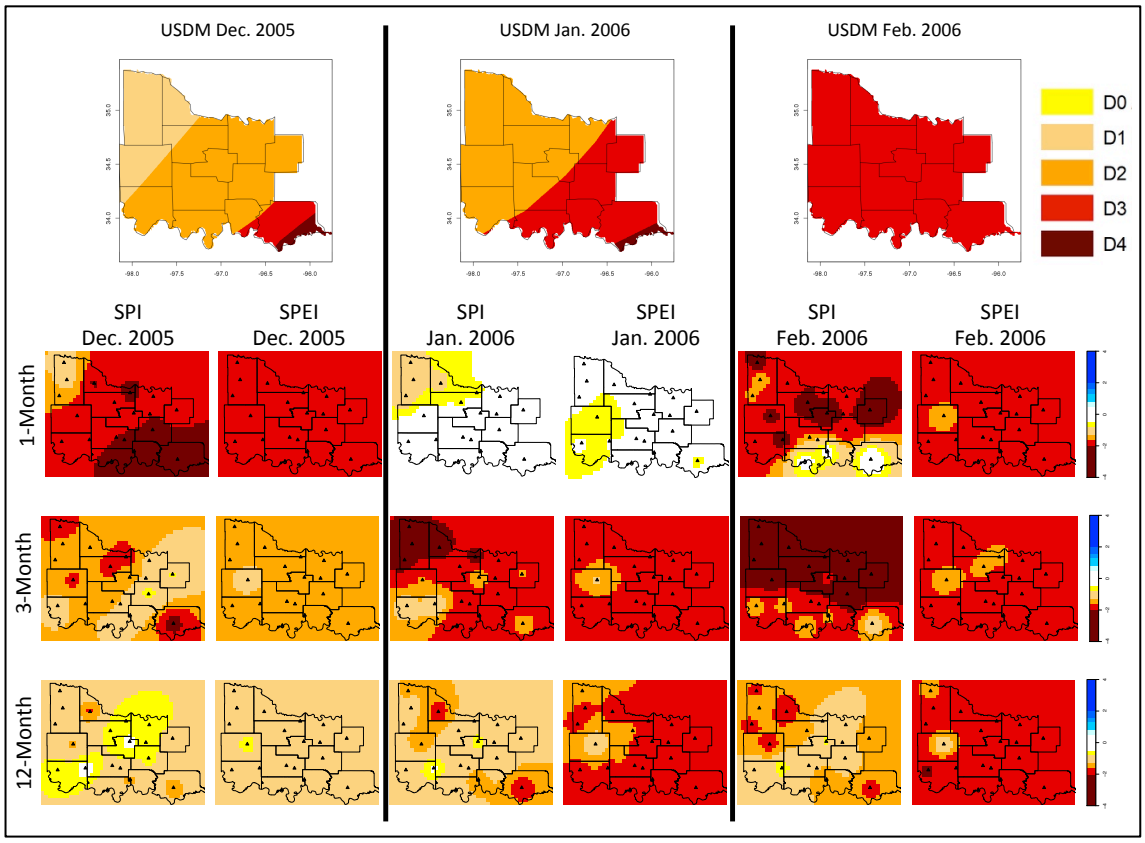

Figure 16: SPI/SPEI over the Chickasaw Nation for December 2005 to February 2006 on 1-, 3-, and 12- month time scales.

4.3 Climate division scale SPI and SPEI

To answer our second research question, we calculated SPI and SPEI values for each month over the entire Chickasaw Nation (hereafter called the Chickasaw dataset), representing a climate division scale (Table 9). Although the RMSEs for the Chickasaw dataset were larger than those for the station-based SPI/SPEI datasets, they are not large differences. The average difference between the Chickasaw dataset and the calculated station-based SPI and SPEI values for all time scales was 0.18, with the largest (smallest) difference being 0.3 (0.1). By our defined threshold, this is not a significant error. With average RMSE below our designated threshold for all times scales, we

conclude that our derived datasets are representative of drought conditions in this region of the U.S.

Table 9: Root Mean Square Error (RMSE) for the SPI and SPEI datasets for the Chickasaw Nation as a whole (climate division-scale) on 1-, 3-, and 12-month time scales

Time Scale	SPI	SPEI
1-month	1.9	1.8
3-month	1.9	1.8
12-month	1.8	1.8

Through this analysis, we were able to determine if drought indices calculated on a climate-division scale were representative of the localized drought severity in that region. While the errors for the climate-division values were larger than those calculated for the station-based data, the RMSE for the Chickasaw dataset was not only below our threshold of a two-category difference, but they were also well below even a one-category difference. As of this time, the Chickasaw Nation still receives climate division-scale information for their decision making processes, and it is important for them to be able to better interpret that information spatially across their region. Our conclusions signify that these data can be reliable for their day-to-day operations, but they will be able to make more meaningful evaluations of their drought conditions with a better understanding of how these impacts vary spatially across the region.

4.4. Drought and Hydrologic Resources

Our third question was to ask how the drought indices reflected the spatial variability of the hydrologic impacts, such as discharge on the rivers and streams. To do so, we first examined whether the temporal patterns in SPI or SPEI values were

reflected in the amount of discharge downstream from the associated Mesonet site. Then we studied these patterns taking into account that there may be lags in the hydrology of the basin, with increases or decreases in streamflow reflected a month or more later than the respective changes in SPI or SPEI values.

For our investigation of the temporal patterns of SPI and SPEI and the spatial variability of the drought impacts on the hydrologic resources from community to community across this region, we conducted a case study of the 2011 – 2015 drought. Our goal was to see if our calculated SPI and SPEI values adequately represented the drought impacts that happened to above-ground water resources in our study area. For this analysis, we utilized 13 hydrologic observing stations (12 rivers and one spring) across the region that had complete records from January 2011 to December 2015. Having a continuous time series through the case study's period of record was essential for the statistical analysis of the hydrologic resources.

First, we performed a qualitative analysis of the datasets to visually assess if the temporal patterns in each hydrologic time series were similar to those in the time series of each drought index. Since it was concluded that all six SPI and SPEI datasets represented drought the same, we only used SPI for this part of the analysis. We observe that the SPI time series moderately reflect the timing and amplitude of the increases and decreases in streamflow discharge. Figure 17 shows an example of this case for the Washita River near Grady, OK. The temporal variability between peaks and minima in discharge and drought index is most noticeable when SPI values are increasing and decreasing concurrently with the percent of normal discharge. It is important to note that peaks in percentage of normal streamflow quickly follow peaks in

SPI, signifying that our values of SPI are improving before the hydrologic resources recover. In addition, minima in the percentage of streamflow are preceded by minima in SPI; meaning drought intensity worsens before it is reflected in the hydrologic resources.

While there are many instances where the timing and amplitude of increase/decrease in the percentage of normal flow are reflected in the SPI plot, instances where there is a well-defined depiction of these patterns are highlighted with orange (decreasing) and blue (increasing) lines in Figure 17. While it is clear that patterns in streamflow are reflected in patterns of SPI time series, there is temporal variability between the two time series. The river and stream discharge observed at this station is affected by precipitation well beyond what is reported at this single Mesonet station and by the Arbuckle-Simpson Aquifer in this region. These hydrologic influences could explain why the fluctuating increases and decreases in streamflow are not as well represented in the SPI time series.

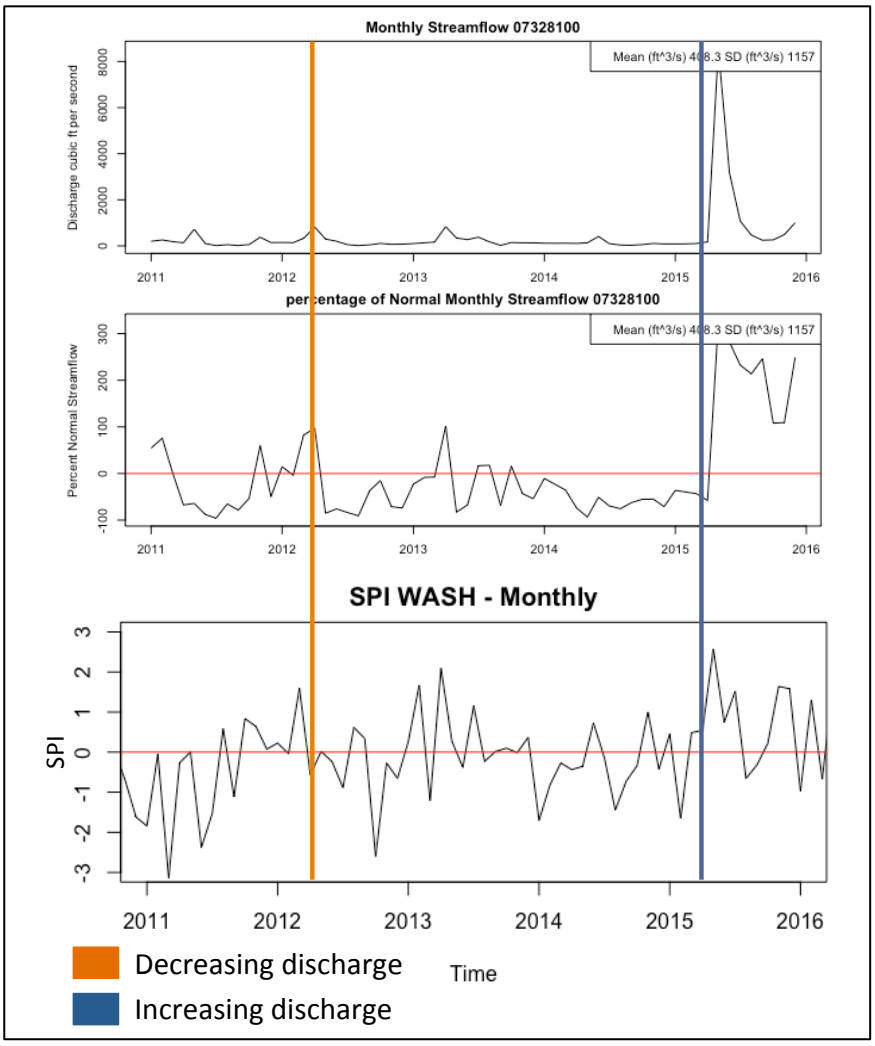

Figure 17: Time series of the Washita River near Grady, OK for monthly discharge, ft^3/s (Top), percentage of normal streamflow (top middle), and SPI 1-month (bottom middle) for the Washington Mesonet station

Next we investigated if there were any spatial patterns connecting SPI and the hydrologic resources in the region. We can see spatial relationships through river systems that contain multiple hydrologic observing stations, such as the Washita River (Fig. 18). This river system, within the bounds of our study area, includes three streamflow stations paired with two different Mesonet stations. This figure displays plots ordered northwest to southeast in downstream stations. Looking at the time series,

we can see the patterns in streamflow are preserved downstream, and the SPI values follow very similar patterns from the Washington Mesonet station (upstream) to the Sulphur Mesonet station (downstream). The timing of the increases in discharge and the timing of increase in SPI values are not identical for each location downstream, but the amplitude of the increase is preserved through each time series. In addition, the magnitude of increasing/decreasing SPI is not identical from the Washington station to the Sulphur station, but the corresponding pattern related to the streamflow time series is continued downstream. However, periods with a sharp decrease in the percentage of normal flow, especially those reflecting a drastic change from positive to negative percentage of flow, are mirrored as decreasing trends in the drought indices.

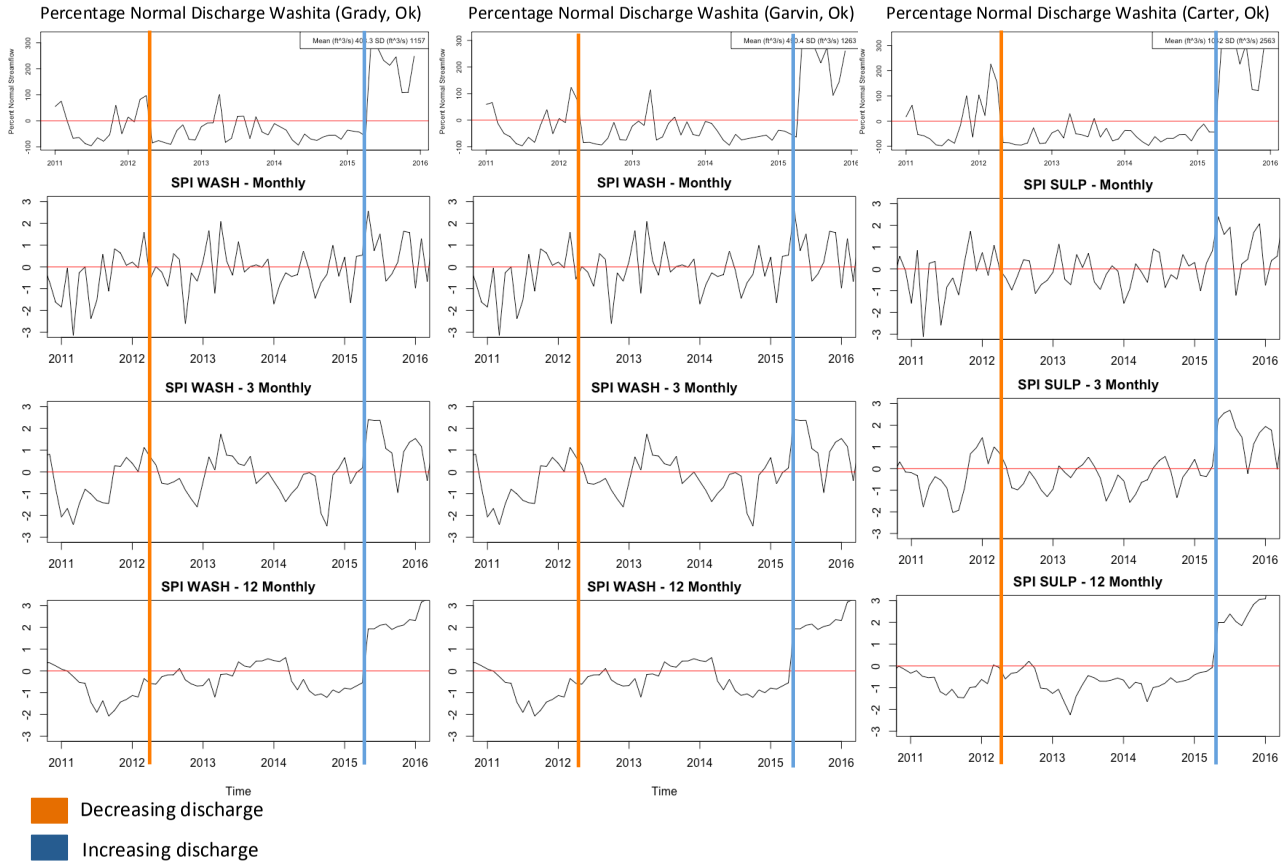

Figure 18: Monthly streamflow and percentage of normal monthly streamflow for the Washita river at three monitoring stations (Grady, Garvin, and Carter, OK, respectively) compared to SPI time series for the Washington (Grady and Garvin) and Sulphur (Carter) Mesonet stations

We continued with our investigation of temporal patterns in SPI values and their indication of discharge downstream from the associated Mesonet site, considering if these patterns are better represented over one of the three calculated SPI time series. Looking more closely at the response of the 1-, 3-, and 12-month SPI values as compared to discharge, periods of continuous, below-average discharge are not reflected by continuously decreasing drought indices. In fact, there are many periods where the 1-month and 3-month SPI values not only increased, but they also showed values above the assigned drought-threshold. There are multiple instances of this pattern across these SPI time series as below-normal discharge persisted in the hydrologic time series.

The time series plots for Antelope Springs (Fig. 19) illustrate this point; while the amplitude of discharge decreases, it is paired with repeated periods of increasing SPI values in the 1- and 3-month time series. The discharge in this spring reaches 0 ft^3/s, (Fall 2012 through Spring 2013, and Fall 2013 until Spring 2015), yet we see positive values of 1- and 3-month SPI. The results from this analysis are consistent with the hydrologic structure in this part of the region as Antelope Springs is recharged exclusively from the sole-source Arbuckle Simpson Aquifer.

Only the SPI 12-month reflects a *continuous* period of drought (negative SPI values indicating dry or drought conditions) while there is no discharge from the spring. SPEI 12-month also reflects more intense drought severity than its 1- and 3-month counterparts, but this time series does reach values above zero during that time frame. From fall 2013 to spring 2015, we not only see that the SPI 12-month values remain below zero, but also that a decreasing trend occurs as the long-term drought conditions

continue through the region. This time scale of SPI allows the user to observe the long-term trends in precipitation. While the shorter time scales depict many instances of drought recovery, the 12-month time scale portrays the underlying lack of precipitation mirrored in the lack recharge to the aquifer, represented by lack of discharge from the spring.

Of the six drought time series, the one that had the best visual representation of the temporal patterns in percent of normal monthly streamflow in the spring was the SPI 12-month time series due to its ability to capture the long-term trends in the region. The river and stream discharges responded more quickly to short duration events, quickly fluctuating between increasing and decreasing values due to its multiple sources of recharge (precipitation runoff and aquifer recharge). We conclude that the long-term impacts of drought on the hydrologic resources across the region are better reflected over long time scales, such as with the 12-month SPI.

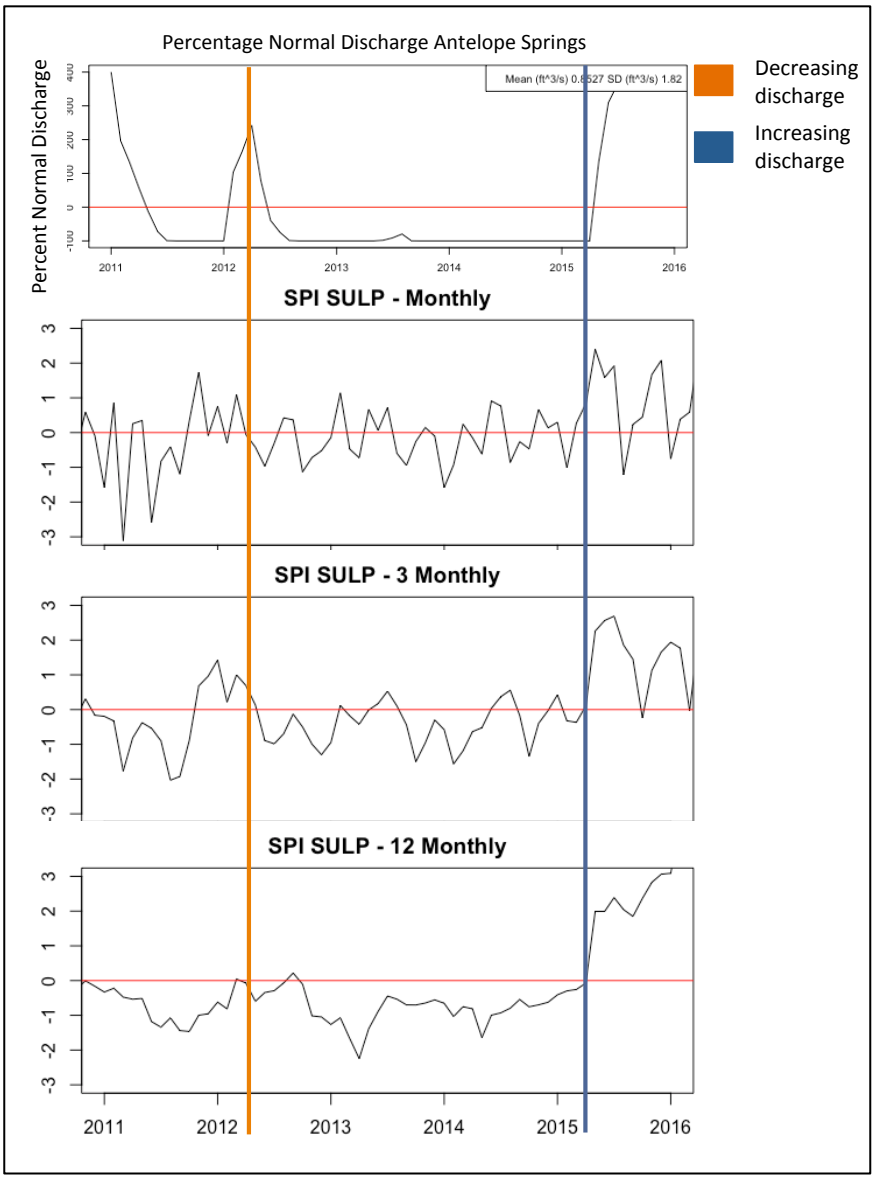

Figure 19: Percentage of normal monthly streamflow (top) as compared to SPI time series over 1-(top-middle), 3-(bottom-middle), and 12-month (bottom) timescales.

Finally, we investigated if our drought indices correlated with the hydrologic impacts from community to community across our region. To do this, we calculated temporal cross-correlations between the streamflow time series for each hydrologic observing site and the SPI and SPEI 1-, 3-, and 12-month time series for its corresponding, upstream Mesonet site. We assigned the dataset of percentage of normal

flow to be our lagged time series to determine their correlation with the calculated drought indices over time. Figure 20 provides an example of the cross correlograms created for each station. This cross correlogram is for the Pennington Creek USGS hydrologic observing site in Reagan, OK, located in the east-central part of the Chickasaw Nation. This streamflow dataset was lagged against SPI/SPEI time series for the Sulphur Mesonet station. The bell shape across the lags indicates that there is a secular trend, i.e. the trends are consistent over time and there are not seasonal or periodic trends being modeled across our correlograms.

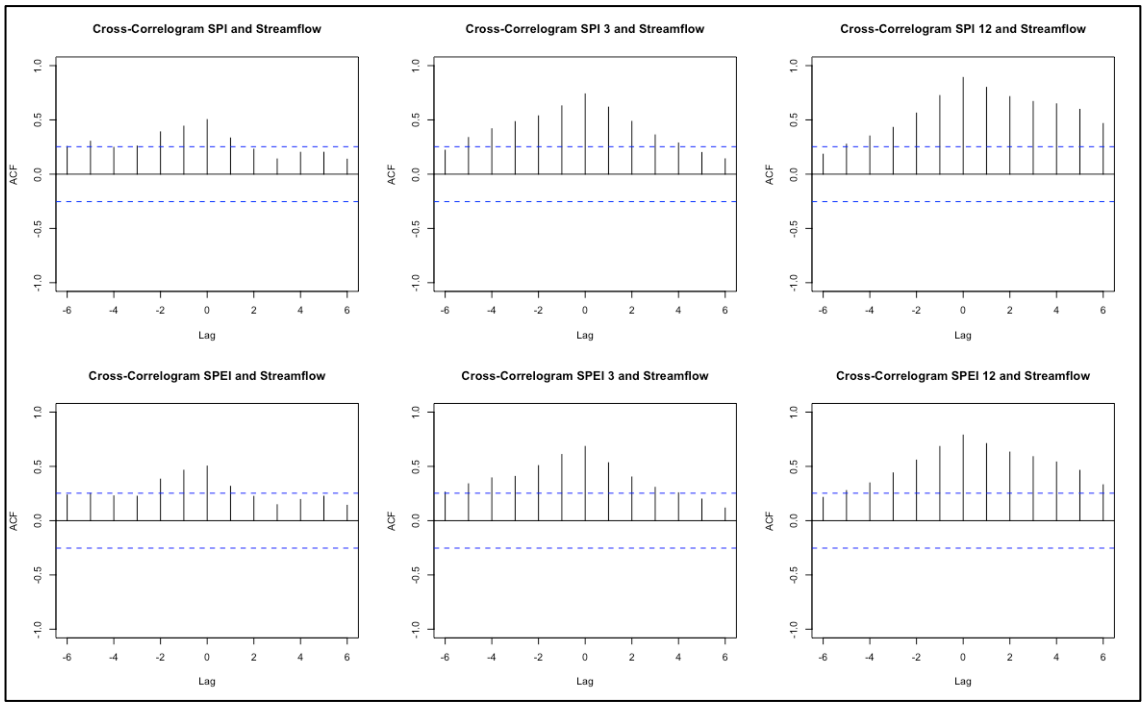

Figure 20: Cross-Correlogram for the Pennington Creek streamflow dataset lagged against the SPI and SPEI 1-, 3-, and 12-month datasets from the Sulphur Mesonet station

Looking at the table of cross-correlations for lag 0, or no time shift, for each dataset in Table 10, we observe that there is a positive cross-correlation between all of our streamflow time series and our drought indices across all time scales. As the lags

increase from 1 to 6 our cross-correlations decrease. The cross-correlations of the SPI and SPEI 1-month time series had the lowest average cross-correlation coefficients for all stations (0.47 and 0.49, respectively), but the cross-correlograms did reflect the same secular trend. The highest correlations for all stations were observed in the 12-month SPI time series, with an average value of 0.73, and the highest cross-correlation coefficient is 0.89 for Pennington Creek. For SPI/SPEI 3-month and 12-month time series, there are high correlations (≥ 0.75) with low lags (1-3); over all the stations, the 3-month time series retained higher correlations left of center with negative lags and the 12-month time series retained higher correlations right of center with positive lags (Fig. 20). The behavior modeled in the 3- and 12-month cross-correlation plots signifies a secular trend, and as the lag increases across the correlogram, correlation decreases.

Table 10: Cross correlation coefficients for lag 0 for correlogram calculated for USGS hydrologic observing site lagged against SPI and SPEI 1-, 3-, and 12-month time series

USGS Hydrologic Observing Site	SPI 1-month	SPI 3-month	SPI 12-month	SPEI 1-month	SPEI 3-month	SPEI 12-month
Murray Antelope	0.32	0.61	0.75	0.34	0.51	0.63
Bryan Blue	0.60	0.81	0.78	0.54	0.73	0.75
Johnston Blue	0.25	0.56	0.83	0.26	0.45	0.66
Murray Honey	0.56	0.70	0.50	0.60	0.71	0.44
Grady little Washita	0.49	0.49	0.64	0.53	0.63	0.60
Jefferson Mud	0.51	0.70	0.61	0.49	0.66	0.46
Johnston Pennington Regan	0.50	0.74	0.89	0.50	0.68	0.79
Love Red Gainesville	0.48	0.71	0.71	0.53	0.70	0.65
Jefferson Red	0.52	0.68	0.69	0.53	0.68	0.61
Murray Rock	0.55	0.76	0.84	0.53	0.67	0.68
Grady Washita	0.42	0.61	0.76	0.48	0.64	0.68
Carter Washita	0.52	0.78	0.79	0.51	0.69	0.64
Garvin Washita	0.43	0.63	0.76	0.48	0.65	0.67

Looking at how the correlations varied spatially across the region, we did not observe any pronounced patterns that were not related to similarities in cross-correlations along the same river or stream. For example, the stations along the Red River (the southern border of our study area) had slightly lower cross-correlation coefficients (0.69 and 0.71) than the other river systems in this study. In contrast, the Washita River (that traverses the center part of the region from northwest to southeast) had some of the highest correlation values (0.76, 0.79, 0.76; Fig. 21). This result is not surprising, as the Red River Basin transports water from well outside the region, thus precipitation and recharge from lands upstream greatly impact the flow. The Washita River Basin is smaller, and it may be more locally responsive to precipitation inputs. Other small streams originating within the region, such as Pennington Creek (Fig. 20), are more highly correlated with SPI because their inputs to recharge are better captured by the data collected at the Mesonet sites due to the fact that these stations are located within the same HUC 12 drainage basin.

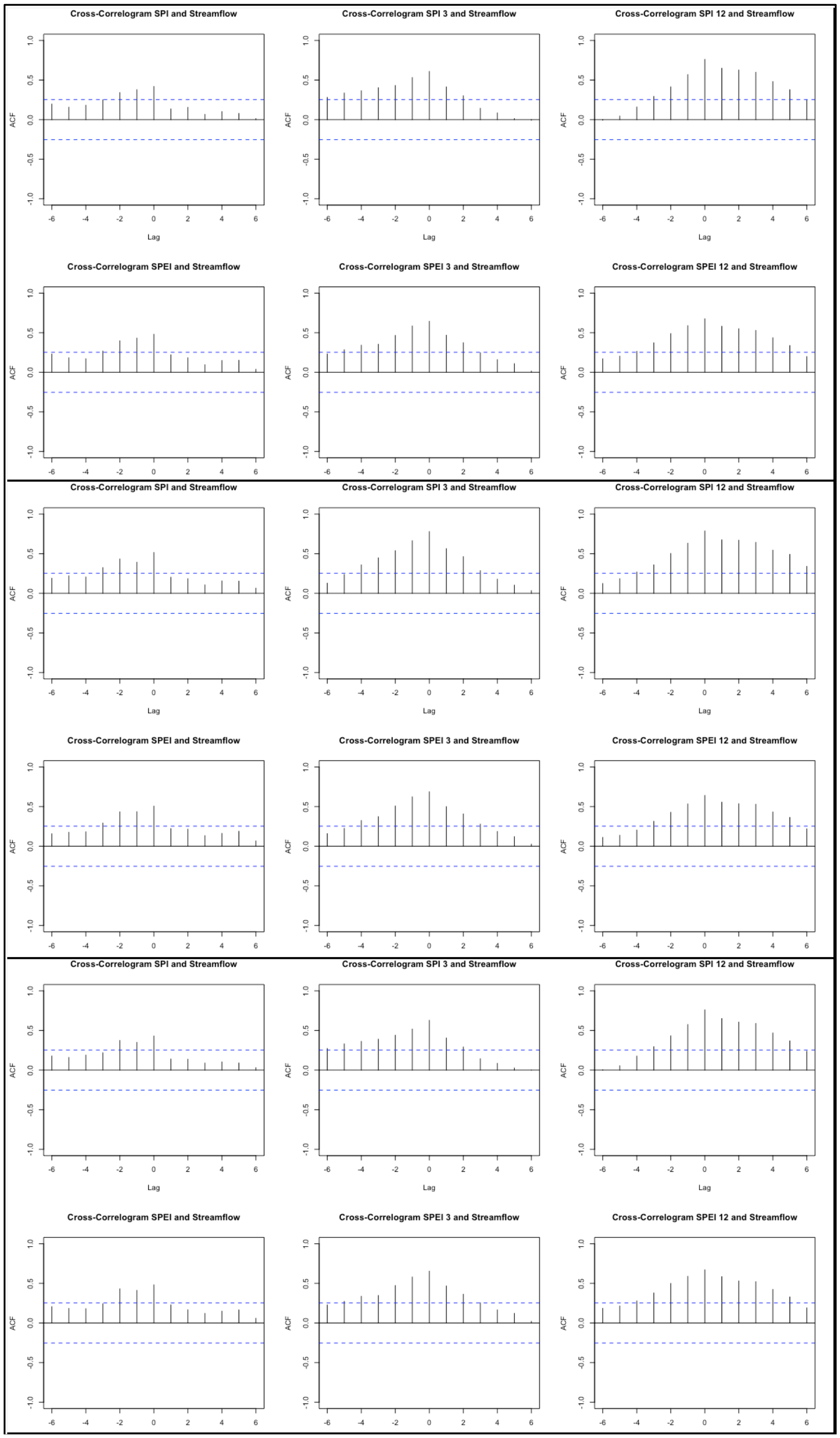

Figure 21: Cross-Correlograms for the Washita river in Grady, Ok paired with Washington station (top), Carter, Ok paired with Sulphur station (middle), and Garvin, Ok paired with Washington station (bottom) for the SPI/SPEI 1-month (left), 3-month (middle), and 12-month (right) time series.

Chapter 5: Discussion and Conclusion

The purpose of this study was to examine the spatial variability of drought and its impacts within the tribal boundaries of the Chickasaw Nation in south-central Oklahoma. In order to examine how the local impacts of drought differ spatially, we determined if our calculated drought indices, SPI and SPEI represented drought differently across 1-, 3-, and 12-month time scales, while also noticing any spatial or seasonal variations. In addition, we assessed if climate-division scale data was representative of the localized impacts over this region. Finally, we conducted a case study of the 2011 – 2015 drought in order to better understand how drought impacts the hydrologic resources from community to community.

We examined if drought severity was better represented with SPI or SPEI, finding that there was not a statistically significant difference between the two datasets for the 1-month, 3-month, or 12-month products. Because the primary difference between SPI and SPEI as measures of drought severity is the inclusion of temperature as a variable within SPEI, we conclude that the effects of temperature do not dominate the development of drought in the study region. Drought is driven principally by precipitation. However, we found statistically significant differences between the SPI and SPEI datasets for the 1-month datasets during fall and spring as well as for the 12-month datasets during fall and summer. Thus, there are times of the year when SPEI values better account for the interaction of warm temperatures with drought development.

We defended our use of SPI and SPEI values for our analysis of drought severity by calculating RMSE for all six SPI and SPEI products against our "truth," the U.S.

Drought Monitor. In aggregate, all SPI and SPEI products had RMSE values below our 2-category threshold, although there were individual months in all of the products when the RMSEs exceeded this threshold. There was greater spatial variability in RMSE for the SPI products as compared to SPEI; however, RMSEs were not necessarily lower for SPI products than for SPEI products. RMSE values were consistently larger in the southern and western portion of the domain, and lower in the northeast part of the region for all station-based SPI and SPEI products. The northeast corner of the Chickasaw Nation holds more of the surface hydrologic resources in the region, including many rivers and streams as well as portions of the Arbuckle-Simpson Aquifer. Variables that measure these resources, such as discharge and groundwater levels, are included in the weekly development of the USDM, perhaps leading to the smaller errors in this area.

Each SPI and SPEI product lends insight to different aspects of drought development. From our boxplots, we concluded that there is more variability within the three SPI datasets than those of SPEI, which was confirmed by the standard deviations of each product. We visually determined that there was not only more temporal variability in SPI from month to month, but there was also more spatial variability from station to station. The 1-month time scales for both SPI and SPEI had the highest spatial variability while the 12-month times scales had the lowest. 1- and 3-month time scales of SPI and SPEI provide short-term information about drought development/recovery, and while the 12-month indices had a lower frequency of drought, they were able to convey the extent of longer duration and more severe droughts.

Finally, we examined if drought impacts the hydrologic resources differently from community to community across this study region. Through this analysis, we found that there is a relationship between the hydrologic variables and our calculated drought indices. Hydrologic patterns are not only reflected through the SPI and SPEI time series, the increasing/decreasing trends in SPI and SPEI are also retained downstream. This feature can be useful information for decision makers when determining the impacts along river systems, as they can expect similar impacts at locations downstream. While the 1- and 3-month calculations of SPI did not represent the hydrologic conditions well across the region, we can verify the impacts of drought on the hydrologic resources with strong correlations between percent of normal streamflow and the SPI 12-month time series. Of the six drought time series, the one that had the highest cross-correlations for all 13 hydrologic time series was the SPI 12-month time series, and calculating the 12-month time series can lend critical information on the long-term trends that are reflected in the hydrologic trends.

5.1 Study limitations

There are limitations with this study, including those related to reliance on the U.S. Drought Monitor to serve as "truth" and sparseness of the hydrological datasets (in both space and time). For example, there are constraints to using the last week of the monthly U.S. Drought Monitor product as a representation of monthly values. Because this product ends on Tuesday of that final week, any changes to drought conditions, such as additional precipitation, increases in streamflow, improvement in SPI, that occur afterwards are not reflected in the product. Yet our 1-month, 3-month, and 12-month products use climate data from every day of the month. Overlooking a gap of up

to six days of data, or up to 20 percent of the month, could explain some of the differences between the SPI/SPEI values and USDM category for the same location. In addition, the USDM generally only changes one category from one week to the next, in both improvement and deterioration of drought conditions. This practice signifies that in some instances, the actual drought conditions may have been different than depicted in the maps during rapid drought onset or decay. Again, this could explain some of the higher RMSEs between SPI and USDM values.

Furthermore, there are limitations surrounding our definition of "truth" in the statistical evaluation of our calculated drought indices. The drought research community has not established any variable or set of variables that definitively defines drought intensity for any point in time, thus we chose what we believe is the best proxy for drought in our designated study area, as it incorporates both objective measures of climate conditions and subjective measures of impacts in its evaluation of drought.

Another limitation to this study is that we paired each discharge observing site with the nearest Mesonet station that was upstream and within the same Hydrologic Unit Code (HUC) 8 drainage basin. There are two smaller scale drainage basin units that can be used: HUC 10 and HUC 12, which provide a more detailed depiction of the runoff region for each stream and its tributaries. Figure 7 shows the HUC-12 boundaries overlain with the USGS stream gauge sites and Mesonet climate-monitoring stations. Many of the USGS observing stations are located at the base of HUC 10 or 12 basins, but the majority of USGS stations do not have a Mesonet station upstream and within those boundaries to pair it to. Our analysis results indicated that Pennington Creek and the Sulphur Mesonet station had the highest correlation of any paired stations, and in

fact, they are located within the same HUC-12 basin. This spatial relationship could explain the high correlation between the two time series. There are many topographic divides present in our study region, especially over the Arbuckle Anticline, that could play a role in lower correlations for stations that are within the same basin in HUC-8 division but not the same HUC-12 division.

5.2 Next steps

There are many ways to continue with this analysis, and methods to incorporate various missing pieces found in the section above. First, we could modify the definition of SPI to match that of USDM in order to observe and change in drought frequency or magnitude within SPI/SPEI. Moving forward we could also look to see how the errors would change if the months of no drought (or RMSE equal to zero), and if there were still no substantial errors in our datasets. These techniques would provide additional insight as to how SPI/SPEI vary from USDM, and could be used in future spatial, temporal, and seasonal analyses of SPI and SPEI in this region.

When considering the method of calculating SPEI, we could incorporate different techniques of calculating evapotranspiration. The other methods of calculating evapotranspiration (Hargreaves and Penman-Monteith) discussed in 2.2.1 have variables that are also measured by the Oklahoma Mesonet, and could be incorporated in the calculation. For example, Hargreaves equation includes solar radiation, and incorporating actual values of solar radiation may lend to a more representative reference evapotranspiration than the potential evapotranspiration calculated by Thornthwaite's equation. From our conclusions, we found that SPI and SPEI did not represent drought differently, so the incorporation of temperature does not play a

significant role in the representation of drought, but additional evapotranspiration calculations may provide additional insight on its influence on drought magnitude.

Moving forward with this study, we could replicate our hydrologic analysis with the other available hydrologic resources within the region. Lake levels from the one lake located within the region were not included as the focus of this study was provide a spatial analysis, but it is important to know how these values correlate with our calculated drought indices. In addition, we could calculate cross-correlograms for soil moisture values measured at each Mesonet station. These values should be highly correlates as they are measured at the same location, removing the possibility of inaccuracies found when pairing USGS stations. Finally, future steps should be taken to include both Mesonet stations and USGS stations located just outside the bounds of the Chickasaw Nation. This could lend additional information into the upstream characteristics between hydrologic recourses and our calculated drought indices.

5.3 Recommendations to the Chickasaw Nation

The results of this study are intended to be useful for the Chickasaw Nation and their Arbuckle-Simpson Aquifer Drought Contingency Plan (the Nations et al. 2017). Specifically, the broader impacts of this study are to provide additional information and guidance to their drought monitoring and response guidelines. Currently, the Nation uses the Palmer Drought Severity Index as their indicator of drought, but this index does not include a temporal component as to how the drought is progressing, which is vital during times of persistent drought. I would recommend that the Nation use 1-, 3-, and 12-month values of SPI calculated at the 19 Mesonet stations within their region. The Arbuckle-Simpson Aquifer Drought Contingency Plan is specific to the hydrologic

resources in the region, so I would recommend using SPI 12-month as their threshold for making response actions. This product would allow them to observe the long-term trends in drought with an index that highly correlates to the other monitored drought triggers (such as streamflow).

I would inform members of the Nation's drought taskforce that while there were higher errors in a climate-division scale dataset, this single value would still be valuable for their analysis, especially if they were unable to produce station-based products. I would still recommend using SPI-12 month, but explain how these errors varied spatially. The climate-division values better represented the northeast corner of their Nation, where the Arbuckle Simpson-Aquifer is located and much of their most important water resources are clustered. As for decisions that may require data in their southwest corner, I would suggest they do some additional evaluations of the hydrologic conditions before making any decisions.

I also would recommend that more research be conducted to better interpret how SPI values compared to the conditions of their hydrologic resources, especially before making decisions based on their prescribed drought stages and response actions in their drought contingency plan. The most important relationships that should be taken into account are the timing of deterioration and improvement in drought conditions and their connection to streamflow discharge. Results show that values of SPI products on all time scales will decrease before the associated drop in streamflow levels. This pattern should be considered when implementing drought stage actions responses, and provides an opportunity for the Nation to be proactive and restrict water usage before the hydrologic resources begin to be depleted. In addition, this knowledge may be vital

information when assigning a Local Drought Stage 3 (Emergency), as this relationship could predict decreases of streamflow in local rivers and streams.

The Chickasaw Nation should also use caution when dismissing drought stages based on increases in hydrologic resources. We found that streamflow discharge will increase before values of SPI increase, and drought conditions may persist for one to two months before values of SPI recover. The Nation may want to wait to reel in the restrictions set in place to off set the impacts of drought until both streamflow and SPI values have improved. This information can better inform their stakeholders on the development of drought, and help the Nation mitigate the impacts of drought in the future.

References

Agnew, C., 2000: Using the SPI to identify drought. Drought Network News (1994-2001). Paper 1. http://digitalcommons.unl.edu/droughtnetnews/1

Allen, R., M. Smith, A. Perrier, and L. S. Pereira, 1994: An update for the definition of reference evapotranspiration. *ICID bulletin*, **43,** 1-34.

Alley, W. M., 1984: The Palmer drought severity index: limitations and assumptions. *Journal of climate and applied meteorology*, **23,** 1100-1109.

American Meteorological Society (AMS), 2018: " Evapotranspiration". Glossary of Meteorology. [Available online at http://glossary.ametsoc.org/wiki/Evapotranspiration]

Arndt, D. S., J. B. Basara, R. A. McPherson, B. G. Illston, G. D. McManus, and D. B. Demko, 2009: Observations of the overland reintensification of Tropical Storm Erin (2007). Bulletin of the American Meteorological Society, 90, 1079-1094.

Babb, R., 2015: Before us, the Chickasaw: Their History is Often Overlooked in the Homeland. *The Journal of Chickasaw History and Culture*, **17,** 60.

Beguería, S., and S. M. Vicente-Serrano, 2013: SPEI: calculation of the standardised precipitation-evapotranspiration index. *R package version*, **1**.

Beguería, S., S. M. Vicente-Serrano, F. Reig, and B. Latorre, 2014: Standardized precipitation evapotranspiration index (SPEI) revisited: parameter fitting, evapotranspiration models, tools, datasets and drought monitoring. *International Journal of Climatology*, **34,** 3001-3023.

Bonaccorso, B., I. Bordi, A. Cancelliere, G. Rossi, and A. Sutera, 2003: Spatial variability of drought: an analysis of the SPI in Sicily. *Water resources management*, **17,** 273-296.

Boone, K. M., R. A. McPherson, M. B. Richman, and D. J. Karoly, 2012: Spatial coherence of rainfall variations using the Oklahoma Mesonet. *International Journal of Climatology*, **32,** 843-853.

Brock, F. V., K. C. Crawford, R. L. Elliott, G. W. Cuperus, S. J. Stadler, H. L. Johnson, and M. D. Eilts, 1995: The Oklahoma Mesonet: a technical overview. *Journal of Atmospheric and Oceanic Technology*, **12,** 5-19.

Brunsdon, C., and L. Comber, 2015: *An introduction to R for spatial analysis and mapping.* Sage.

Christenson, S., N. I. Osborn, C. R. Neel, J. R. Faith, C. D. Blome, J. Puckette, and M. P. Pantea, 2011: Hydrogeology and simulation of groundwater flow in the Arbuckle-

Simpson aquifer, south-central Oklahoma.

Dai, A., K. E. Trenberth, and T. T. Qian, 2004: A global dataset of Palmer Drought Severity Index for 1870-2002: Relationship with soil moisture and effects of surface warming. *Journal of Hydrometeorology*, **5,** 1117-1130.

Dai, A. G., 2011: Drought under global warming: a review. *Wiley Interdisciplinary Reviews-Climate Change*, **2,** 45-65.

Drought Impacts Reporter (DIR) 2018. National Drought Mitigation Center (NDMC), an the University of Nebraska, Lincoln. [Available online at http://droughtreporter.unl.edu/map/]

Edwards, D. C., 1997: Characteristics of 20th century drought in the United States at multiple time scales.

Faith, J. R., and Coauthors, 2010: Three-dimensional geologic model of the Arbuckle-Simpson Aquifer, south-central Oklahoma2331-1258.

Fiebrich, C. A., D. L. Grimsley, R. A. McPherson, K. A. Kesler, and G. R. Essenberg, 2006: The value of routine site visits in managing and maintaining quality data from the Oklahoma Mesonet. J. Atmos. Oceanic Technol., 23, 406–416.

Fiebrich, C. A., C. R. Morgan, A. G. McCombs, P. K. Hall, Jr., and R. A. McPherson, 2010: Quality assurance procedures for mesoscale meteorological data. J. Atmos. Oceanic Technol., 27, 1565–1582.

Fiorillo, F., and A. Doglioni, 2010: The relation between karst spring discharge and rainfall by cross-correlation analysis (Campania, southern Italy). *Hydrogeology Journal*, **18,** 1881-1895.

Fiorillo, F., and F. M. Guadagno, 2010: Karst spring discharges analysis in relation to drought periods, using the SPI. *Water resources management*, **24,** 1867-1884.

Guttman, N. B., J. R. Wallis, and J. Hosking, 1992: SPATIAL COMPARABILITY OF THE PALMER DROUGHT SEVERITY INDEX1. Wiley Online Library.

Guttman, N. B., 1998: Comparing the palmer drought index and the standardized precipitation index1. Wiley Online Library.

Guttman, N. B., 1999: Accepting the standardized precipitation index: a calculation algorithm. *JAWRA Journal of the American Water Resources Association*, **35,** 311-322.

Hargreaves, G. H., and Z. A. Samani, 1985: Reference crop evapotranspiration from temperature. *Applied engineering in agriculture*, **1,** 96-99.

Hayes, M. J., M. D. Svoboda, D. A. Wilhite, and O. V. Vanyarkho, 1999: Monitoring the 1996 drought using the standardized precipitation index. *Bulletin of the American meteorological society*, **80,** 429-438.

Hayes, M. J., 2000: Revisiting the SPI: clarifying the process.

Hayes, M., M. Svoboda, N. Wall, and M. Widhalm, 2011: The Lincoln declaration on drought indices: universal meteorological drought index recommended. *Bulletin of the American Meteorological Society*, **92,** 485-488.

Heim Jr, R. R., 2002: A review of twentieth-century drought indices used in the United States. *Bulletin of the American Meteorological Society*, **83,** 1149-1165.

Illston, B. G., and J. B. Basara, 2003: Analysis of short-term droughts in Oklahoma. *Eos*, **84,** 157,161.

Illston, B. G., and Coauthors, 2008: Mesoscale monitoring of soil moisture across a statewide network. *Journal of Atmospheric and Oceanic Technology*, **25,** 167-182.

Intergovernmental Panel on Climate Change (IPCC), 2014: climate change 2014: synthesis report. Contribution of Working Groups I

Karl, T. R., 1986: The sensitivity of the Palmer drought severity index and Palmer's Z-index to their calibration coefficients including potential evapotranspiration. *Journal of Climate and Applied Meteorology*, **25,** 77-86.

Keyantash, J., and J. A. Dracup, 2002: The quantification of drought: an evaluation of drought indices. *Bulletin of the American Meteorological Society*, **83,** 1167-1180.

Khalili, D., T. Farnoud, H. Jamshidi, A. A. Kamgar-Haghighi, and S. Zand-Parsa, 2011: Comparability analyses of the SPI and RDI meteorological drought indices in different climatic zones. *Water resources management*, **25,** 1737-1757.

Köppen, W., 1936: Das Geographische System der Klimate, Handbuch der Klimatologie W. Köppen, R. Geiger.

Lawrimore, J., R. R. H. Jr., M. Svoboda, V. Swail, and P. J. Englehart, 2002: BEGINNING A NEW ERA OF DROUGHT MONITORING ACROSS NORTH AMERICA. *Bulletin of the American Meteorological Society*, **83,** 1191-1192.

Looper, J. P., B. E. Vieux, and M. A. Moreno, 2012: Assessing the impacts of precipitation bias on distributed hydrologic model calibration and prediction accuracy. *Journal of Hydrology*, **418,** 110-122.

Lorenzo-Lacruz, J., S. M. Vicente-Serrano, J. I. López-Moreno, S. Beguería, J. M. García-Ruiz, and J. M. Cuadrat, 2010: The impact of droughts and water management on various hydrological systems in the headwaters of the Tagus River (central Spain). *Journal of Hydrology*, **386,** 13-26.

Malone, J. H., 1922: *The Chickasaw Nation: A short sketch of a noble people.* JP Morton, incorporated.

McKee, T. B., N. J. Doesken, and J. Kleist, 1993: The relationship of drought frequency and duration to time scales. *Proceedings of the 8th Conference on Applied Climatology*, American Meteorological Society Boston, MA, 179-183.

McPherson, R. A., and Coauthors, 2007: Statewide monitoring of the mesoscale environment: A technical update on the Oklahoma Mesonet. *Journal of Atmospheric and Oceanic Technology*, **24,** 301-321.

McPherson, R. A., J. D. Lane, K. C. Crawford, and W. G. McPherson, 2011: A climatological analysis of heatbursts in Oklahoma (1994–2009). *International Journal of Climatology*, **31,** 531-544.

Milly, P. C. D., K. A. Dunne and A. V. Vecchia, 2005: Global pattern of trends in streamflow and water availability in a changing climate. *Nature*, **438,** 347.

Milly, P. C., J. Betancourt, M. Falkenmark, R. M. Hirsch, Z. W. Kundzewicz, D. P. Lettenmaier, and R. J. Stouffer, 2008: Stationarity is dead: Whither water management? *Science*, **319,** 573-574.

Mishra, A. K., and V. P. Singh, 2010: A review of drought concepts. *Journal of Hydrology*, **391,** 202-216.

National Centers for Environmental Information (NCEI) U.S. Billion-Dollar Weather and Climate Disasters (2018). National Oceanic and Atmospheric Administration (NOAA) https://www.ncdc.noaa.gov/billions/

National Oceanic and Atmospheric Administration (NOAA), 2018. North American Drought Monitor (NADM), National Centers for Environmental Information. [Available online at: https://www.ncdc.noaa.gov/temp-and-precip/drought/nadm/]

The Choctaw and Chickasaw Nations (The Nations), Duane Smith and Associates, and AquaStrategies, Inc, 2017: Arbuckle-Simpson Aquifer Drought Contingency Plan.

Oklahoma Water Resources Board (OWRB), 2003. The Arbuckle Simpson Hydrology Study: Management and Protection of an Oklahoma Water Resource. [Available online at:
http://www.owrb.ok.gov/studies/groundwater/arbuckle_simpson/arbuckle_study.php]

Oklahoma Water Resources Board (OWRB), 2018. Oklahoma Surface Water Resources, Streams of Oklahoma. [Available online at: http://www.owrb.ok.gov/maps/pdf_map/SW%20Streams.pdf]

Oklahoma Climatological Survey (OCS), 2018. Normal Annual Precipitation. [Available online at: http://climate.ok.gov/index.php/climate/map/normal_annual_precipitation/oklahoma_climate]

Otkin, J. A., M. Svoboda, E. D. Hunt, T. W. Ford, M. C. Anderson, C. Hain, and J. B. Basara, 2017: Flash droughts: A review and assessment of the challenges imposed by rapid onset droughts in the United States. *Bulletin of the American Meteorological Society*.

Palmer, W. C., 1965: *Meteorological drought.* Paper No. 45. Washington, DC: US Department of Commerce. *Weather Bureau*, 59.

Pebesma, E.J., 2003. GStat User's Manual. Utrecht University. [Available online at: http://www.gstat.org/gstat.pdf]

Peel, M. C., B. L. Finlayson, and T. A. McMahon, 2007: Updated world map of the Köppen-Geiger climate classification. *Hydrology and earth system sciences discussions*, **4,** 439-473.

Peters, A. J., E. A. Walter-Shea, L. Ji, A. Vina, M. Hayes, and M. D. Svoboda, 2002: Drought monitoring with NDVI-based standardized vegetation index. *Photogrammetric engineering and remote sensing*, **68,** 71-75.
Rhee, J., J. Im, and G. J. Carbone, 2010: Monitoring agricultural drought for arid and humid regions using multi-sensor remote sensing data. *Remote Sensing of Environment*, **114,** 2875-2887.

Potop, V., 2011: Evolution of drought severity and its impact on corn in the Republic of Moldova. *Theoretical and Applied Climatology*, **105,** 469-483.

Raziei, T., B. Saghafian, A. A. Paulo, L. S. Pereira, and I. Bordi, 2009: Spatial patterns and temporal variability of drought in western Iran. *Water Resources Management*, **23,** 439-455.

Rim, C. S., 2013: The implications of geography and climate on drought trend. *International Journal of Climatology*, **33,** 2799-2815.

RStudio Team, 2016: RStudio: Integrated Development Environment for R. *RStudio Inc, Boston, Massachusetts***,** 74.

Ryberg, K.R. and Vecchia, A.V., 2012, waterData—An R package for retrieval, analysis, and anomaly calculation of daily hydrologic time series data, version 1.0: *U.S. Geological Survey Open-File Report 2012–*1168, 8 p. [Available online at: http://pubs.usgs.gov/of/2012/1168/.]

Shafer, M. A., C. A. Fiebrich, D. S. Arndt, S. E. Fredrickson, and T. W. Hughes, 2000: Quality assurance procedures in the Oklahoma Mesonetwork. *Journal of Atmospheric and Oceanic Technology*, **17,** 474-494.

Smith, A. B., and R. W. Katz, 2013: US billion-dollar weather and climate disasters: data sources, trends, accuracy and biases. *Natural hazards*, **67,** 387-410.

Smith, A. B., and J. L. Matthews, 2015: Quantifying uncertainty and variable sensitivity within the US billion-dollar weather and climate disaster cost estimates. *Natural Hazards*, **77,** 1829-1851.

Soulé, P. T., 1992: Spatial patterns of drought frequency and duration in the contiguous USA based on multiple drought event definitions. *International Journal of Climatology*, **12,** 11-24.

Svoboda, M., and Coauthors, 2002: The drought monitor. *Bulletin of the American Meteorological Society*, **83,** 1181-1190.

Tang, C., and T. C. Piechota, 2009: Spatial and temporal soil moisture and drought variability in the Upper Colorado River Basin. *Journal of Hydrology*, **379,** 122-135.

Thornthwaite, C. W., 1948: An approach toward a rational classification of climate. *Geographical review*, **38,** 55-94.

Towler, E., and H. Lazrus, 2016: Increasing the usability of drought information for risk management in the Arbuckle Simpson Aquifer, Oklahoma. *Climate Risk Management*, **13,** 64-75.

Tsakiris, G., and H. Vangelis, 2005: Establishing a drought index incorporating evapotranspiration. *European Water*, **9,** 3-11.

Turner, R., 2007: The deldir package. [Available online at: http://btr0x2.rz.uni-bayreuth.de/math/statlib/R/CRAN/doc/packages/deldir.pdf]

Umran Komuscu, A., 1999: Using the SPI to analyze spatial and temporal patterns of drought in Turkey. *Drought Network News (1994-2001)***,** 49.

U.S. Drought Monitor (USDM), 2018(a). National Drought Mitigation Center (NDMC), the U.S. Department of Agriculture (USDA) and the National Oceanic and Atmospheric Administration (NOAA). [Available online at http://droughtmonitor.unl.edu]

U.S. Drought Monitor (USDM), 2018(b): GIS Data Archive 2000-2017. National Drought Mitigation Center (NDMC), the U.S. Department of Agriculture (USDA) and the National Oceanic and Atmospheric Administration (NOAA). [Available online at http://droughtmonitor.unl.edu/MapsAndData/GISData.aspx]

U.S. Environmental Protection Agency (EPA), 2006. Terms of Environment: Glossary, Abbreviations, and Acronyms. [Available online at: http://infohouse.p2ric.org/ref/01/00402/sterms.html]

U.S. Environmental Protection Agency (EPA), 2018. Ecoregion Download Files by State - Region 6. National Health and Environmental Effects Research Laboratory. [Available online at: https://www.epa.gov/eco-research/ecoregion-download-files-state-region-6#pane-34]

U.S. Geologic Survey (USGS), 2018. USGS Water Data for USA: National Water Information System. U.S Department of the Interior. [Available online at: https://waterdata.usgs.gov/nwis]

Vangelis, H., M. Spiliotis, and G. Tsakiris, 2011: Drought severity assessment based on bivariate probability analysis. *Water resources management*, **25,** 357-371.

Vicente-Serrano, S. M., 2006: Differences in spatial patterns of drought on different time scales: an analysis of the Iberian Peninsula. *Water Resources Management*, **20,** 37-60.

Vicente-Serrano, S. M., S. Beguería, and J. I. López-Moreno, 2010: A multiscalar drought index sensitive to global warming: the standardized precipitation evapotranspiration index. *Journal of climate*, **23,** 1696-1718.

Vicente-Serrano, S. M., and Coauthors, 2012: Performance of drought indices for ecological, agricultural, and hydrological applications. *Earth Interactions*, **16,** 1-27.

Viessman, W., G. L. Lewis, and J. W. Knapp, 1989: Introduction to hydrology.

Wheaton, E., S. Kulshreshtha, V. Wittrock, and G. Koshida, 2008: Dry times: hard lessons from the Canadian drought of 2001 and 2002. *The Canadian Geographer/Le Géographe canadien*, **52,** 241-262.

Wilhite, D. A., M. D. Svoboda, and M. J. Hayes, 2007: Understanding the complex impacts of drought: a key to enhancing drought mitigation and preparedness. *Water resources management*, **21,** 763-774.

Wilks, Daniel S., 1995, *Statistical Methods in the Atmospheric Sciences: an Introduction,* Academic Press, 467 pp.

Zargar, A., R. Sadiq, B. Naser, and F. I. Khan, 2011: A review of drought indices. *Environmental Reviews*, **19,** 333-349.

Zhai, J., B. Su, V. Krysanova, T. Vetter, C. Gao, and T. Jiang, 2010: Spatial variation and trends in PDSI and SPI indices and their relation to streamflow in 10 large regions of China. *Journal of Climate*, **23,** 649-663.

Ziolkowska, J. R., and Coauthors, 2017: Benefits and Beneficiaries of the Oklahoma Mesonet: A Multisectoral Ripple Effect Analysis. *Weather, Climate, and Society*, **9,** 499-519.